



Metal oxide-based nanocomposites as advanced electrode materials for enhancing electrochemical performance of Supercapacitors: A comprehensive review

Dadaso D Mohite^a, Sachin S Chavan^{a,*}, Prasad E Lokhande^b, Kailasnath B Sutar^a, Sumit Dubal^c, Udaybhaskar Rednam^b, Bandar Ali Al-Asbahi^d, Yedluri Anil Kumar^e

^a Bharati Vidyapeeth (Deemed to be University) College of Engineering, Pune-411043 India

^b Departamento de Mecánica, Facultad de Ingeniería, Universidad Tecnológica Metropolitana, Santiago, Chile

^c Symbiosis Skills and Professional University, Pune 412101 India

^d Department of Physics & Astronomy, College of Science, King Saud University, P.O. Box 2455, Riyadh-11451 Saudi Arabia

^e Saveetha School of Engineering, Saveetha Institute of Medical and Technical Sciences, Saveetha University, Chennai 602105, Tamil Nadu, India

ARTICLE INFO

Keywords:

Electrochemical Performance
Metal Oxide
Nanocomposites
Supercapacitors

ABSTRACT

In recent years, the escalating use of nonrenewable fossil fuels has emerged as a significant threat to global sustainability, prompting the need for renewable, cost-effective, and eco-friendly energy storage solutions. Supercapacitors (SCs) are notable for their high power density (PD), cycle stability, and swift charge/discharge rates, although they fall short in energy density (ED) compared to traditional batteries. The performance of SCs is greatly influenced by the electrode materials used, highlighting the importance of material innovation in tackling the challenges posed by increasing fossil fuel consumption. Transition metal oxides (TMOs), known for their redox activity in energy storage, have been thoroughly investigated for their exceptional specific capacitance, which ranges from 100 to 2000F g⁻¹, surpassing that of electrical double-layer capacitors (EDLCs). TMOs such as ruthenium oxide (RuO₂), manganese oxide (MnO₂), nickel oxide (NiO), cobalt oxide (Co₃O₄), tin oxide (SnO₂), zinc oxide (ZnO), tungsten oxide (WO₃), and vanadium pentoxide (V₂O₅) are widely researched for their high theoretical capacitance, affordability, and longevity. This review emphasizes the groundbreaking potential of metal oxide nanocomposites (NCs) formed by combining them with graphene, carbon nanotubes (CNTs), and polymers, leading to synergistic enhancements in electrical conductivity, surface area, and charge storage capacity. This thorough review not only presents an in-depth analysis of current research but also sheds light on potential future developments, contributing to the ongoing progress in the field of advanced electrode materials for energy storage.

1. Introduction

Supercapacitors (SCs), also commonly known as electrochemical capacitors, have garnered immense interest as versatile energy storage technology that bridges the gap between conventional capacitors and batteries [1,2,3]. Their unique ability to provide high PD, rapid charge-discharge kinetics, and extended cycle life has led to their integration into a variety of applications, from portable electronics and renewable energy systems to electric vehicles and grid stabilization [4–3]. The outstanding performance of SCs is intricately linked to the properties of their constituent electrode materials, which play an important role in finding the ED and PD, as well as overall device efficiency [5]. Among

the diverse array of materials explored for SC electrodes, MOs have emerged as particularly promising candidates. These MOs exhibit attractive redox properties, abundant electrochemical sites, and the potential for reversible Faradaic reactions, making them ideal contenders for efficient energy storage [6]. However, to fully harness the inherent capabilities of MOs, researchers have sought to enhance their electrochemical performance through innovative strategies [7].

In fuel cells and batteries, energy is generated through chemical redox reactions, while SCs, release energy via ion diffusion at the electrode-electrolyte interface, forming electrostatic double layers [2]. SCs serve as an intermediary between conventional capacitors, which offer high PD but low ED, and batteries, which provide high ED but low PD

* Corresponding author.

E-mail address: sschavan@bvucoep.edu.in (S.S. Chavan).

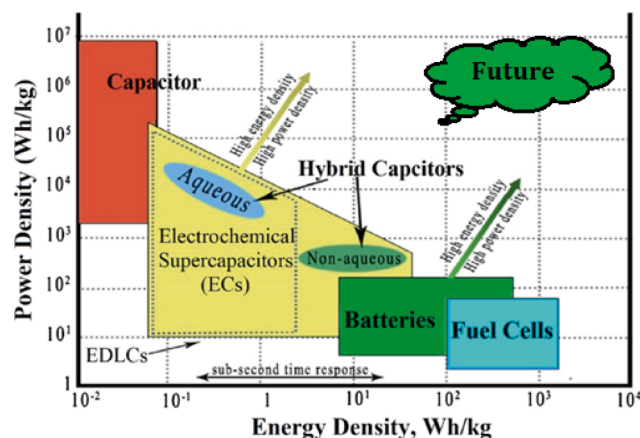


Fig. 1. Ragone plot representing various energy storage systems. Reproduced from Ref. [9]. [copyright with permission from Elsevier, 2024].

[4,8]. They are favored over batteries due to their rapid charging capability and faster energy delivery. Moreover, SCs exhibit durability, stability, and a commendable lifespan. This review highlights that a strategic choice of electrolyte and electrode materials can address the relatively low ED of the system. Fig. 1 illustrates a Ragone plot and visually compares the ED and PD of various energy storage systems.

The concept of NCs, wherein MOs are combined with other nanomaterials, has garnered considerable attention due to its potential to synergistically enhance various electrode characteristics [6,10]. In particular, the integration of MOs with materials such as graphene, CNTs, and polymers has demonstrated remarkable improvements in electrical conductivity, surface area, and charge storage capacity [11,12]. These NCs not only address the inherent limitations of MOs, such as low electrical conductivity and sluggish charge transfer kinetics but enable fine-tuning characteristics like capacitance and ED in SC electrodes to achieve optimized performance [7,13,14].

Fig. 2 presents a classification scheme for SCs based on the materials used for their electrode components [15]. This visual representation offers a systematic categorization of SC technologies, emphasizing the critical role that electrode materials play in determining device

performance. By categorizing SCs according to electrode material, Fig. 2 provides a clear and informative reference for understanding the diverse landscape of SC technologies and their relationship to material selection. The classification system facilitates a comprehensive view of the field, enabling researchers and engineers to explore and compare various electrode materials and their implications for SC design and performance.

This review offers a critical perspective on MO-based NCs as a transformative class of electrode materials for SCs. It addresses the inherent limitations of conventional electrode materials, such as restricted rate capability due to low conductivity. The review explores how these NCs can synergistically combine the properties of MOs with other materials at the nanoscale. This approach has the potential to deliver enhanced electrochemical performance through increased surface area for improved capacitance, better conductivity for faster charge-discharge, and improved structural stability for extended cyclability. By delving into various types of metal oxide NCs, their synthesis methods, and recent advancements, this review provides valuable insights for researchers and engineers in the development of next-generation high-performance SCs.

2. TMO-based materials and their composites for SC electrode

MO-based electrode materials have emerged as a cornerstone for achieving high-performance SCs, offering a compelling blend of electrochemical reactivity, stability, and cost-effectiveness [10]. These materials, characterized by their inherent redox properties, facilitate reversible Faradaic reactions that underlie efficient charge storage and release processes [16]. MOs encompass a diverse range of compounds, including RuO_2 , MnO_2 , WO_3 , V_2O_5 , Co_3O_4 , and NiO , each with distinctive electrochemical characteristics [12]. Their ability to undergo controlled redox transformations allows for significant pseudocapacitance, where energy is stored by highly reversible electron transfer processes (redox reactions) on the surface of the electrode where it contacts the electrolyte [16]. This imparts MO-based electrode materials with the capacity to achieve high ED, rendering them vital components in bridging the gap between traditional capacitors and energy-dense batteries. Fig. 3 presents a theoretical comparison of C_{sp} values for different TMOs.

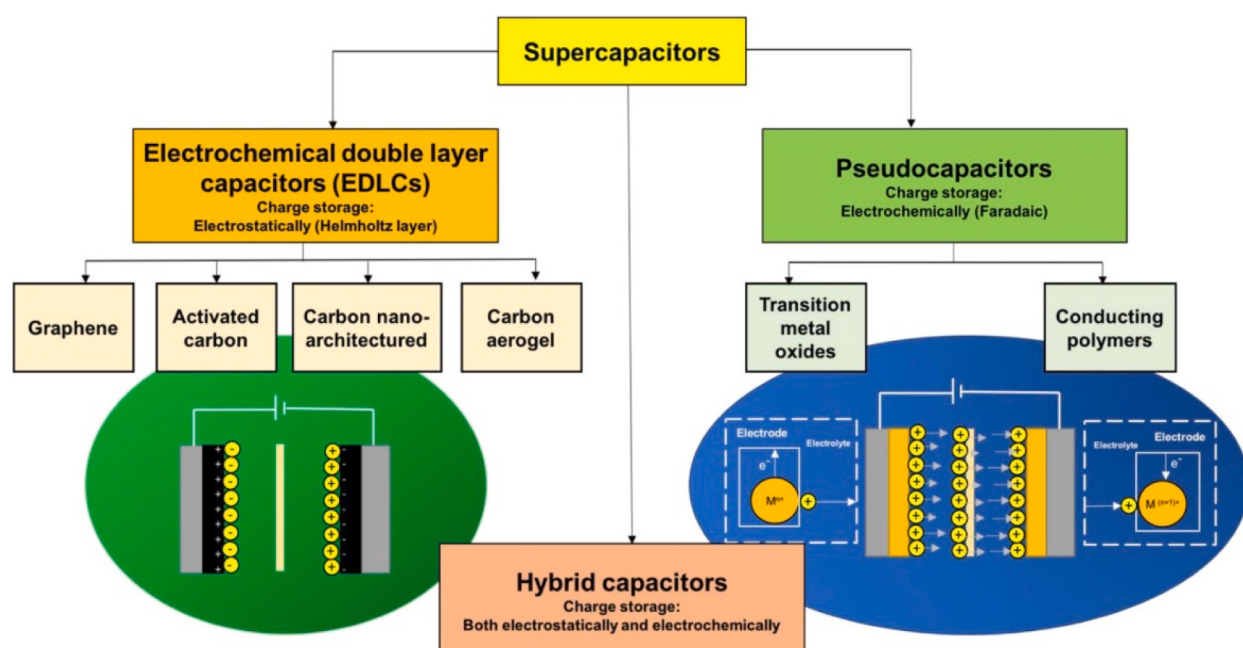


Fig. 2. Classification of SCs according to material used for electrode. Reproduced from Ref. [15]. [Copyright with permission from Elsevier, 2024].

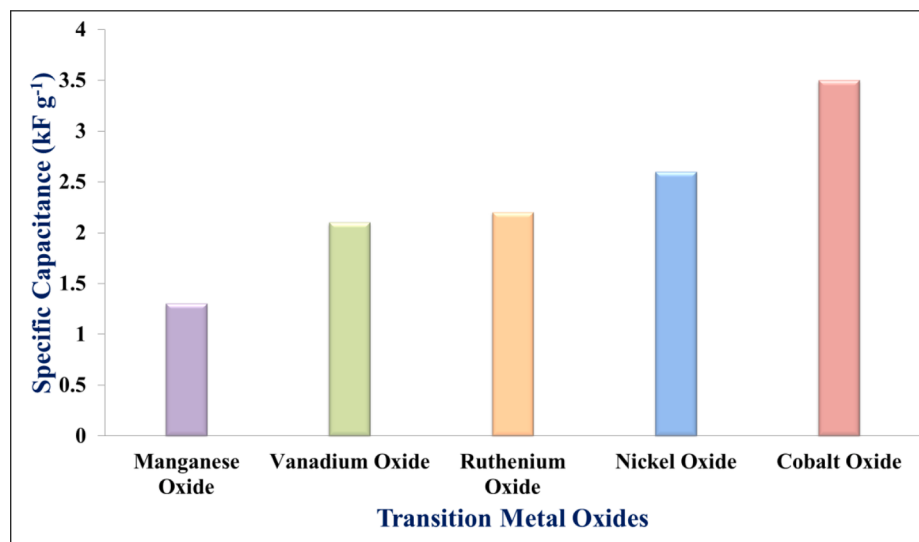


Fig. 3. Comparative study of theoretical C_{sp} in TMO materials [17].

The efficacy of MO-based electrode materials is further amplified through the integration of nanoscale engineering and design. NCs formed by combining MOs with materials like graphene, CNTs, and polymers introduce unprecedented avenues for enhancing charge storage capabilities [5]. These nanomaterial additives contribute to enhanced electrical conductivity, enlarged surface area, and improved charge transport kinetics. The resulting composite structures facilitate rapid ion diffusion, reducing the diffusion path lengths and enabling efficient charge transfer processes. Additionally, the synergistic interactions between MOs and nanomaterials mitigate issues related to volume expansion during cycling, enhancing cycle stability and prolonging the operational lifespan of SC electrodes [18]. As a consequence, MOs-based electrode materials, enriched by NC integration, stand poised to revolutionize energy storage applications across a spectrum of fields, including portable electronics, renewable energy systems, transportation, and grid-level energy management. By harnessing the synergistic capabilities of MOs and nanomaterials, these advanced electrode materials lay the foundation for a more energy-efficient and sustainable future.

MO-based NCs for SC applications represent a pioneering approach that merges the unique properties of MOs with various nanomaterials to create advanced electrode materials. These NCs leverage the high C_{sp} and redox activity of MOs, such as RuO_2 , MnO_2 , and Co_3O_4 , in conjunction with the exceptional characteristics of materials like graphene, CNTs, and conducting polymers. The incorporation of nanomaterials within MOs introduces several advantageous features. Graphene and CNTs enhance electrical conductivity, facilitating efficient charge transport and rapid energy storage. Conducting polymers contribute electrical conductivity and mechanical flexibility, allowing for electrode flexibility and reduced stress during cycling [19]. The unique properties of these nanomaterials synergize with the redox behavior of MOs, resulting in composites that exhibit enhanced C_{sp} , high rate capability, and long-term cycling stability [20].

The synthesis of MO-based NCs involves a range of techniques, including sol-gel methods, hydrothermal synthesis, and electrochemical deposition. Achieving a uniform dispersion of nanomaterials within the MO matrix is crucial to engineering the composite electrode for maximized electrochemical characteristics [21]. These NCs find application in SCs, offering higher ED and PD relative to traditional electrode materials. Their versatility spans various domains, from portable electronics to grid-level energy storage, offering efficient energy storage solutions. As research continues to advance, the optimization of NC compositions, structures, and synthesis techniques will pave the way for

the widespread adoption of MO-based NCs, driving the evolution of SC technology and meeting the demands of modern energy storage systems [22,23].

2.1. Ruthenium oxide (RuO_2)

RuO_2 exhibits a unique confluence of properties that position it as a frontrunner for pseudocapacitive electrode materials. Notably, its theoretical capacitance of 2000 Fg^{-1} signifies exceptional charge storage capability. Furthermore, RuO_2 facilitates rapid Faradaic redox reactions, enhancing overall energy storage efficiency. Additionally, good electrical conductivity ensures efficient charge transport within the electrode. RuO_2 demonstrates high chemical and thermal stability, making it suitable for demanding operational environments. Finally, the wide voltage window offered by RuO_2 allows for greater flexibility in SC design. While these properties establish RuO_2 as a highly desirable electrode material [1,24], its large-scale application remains limited due to the significant cost associated with ruthenium.

- RuO_2 -Based Composite Electrodes

RuO_2 -based composite electrodes offer a promising strategy to address two key challenges: maximizing RuO_2 utilization and reducing overall electrode cost [25]. These composites leverage the synergistic effects between RuO_2 and other materials to achieve enhanced electrochemical performance. Researchers have explored various configurations, including metal sulfide- RuO_2 , MO- RuO_2 , carbon material- RuO_2 , and even multi-component combinations [25–30]. In a study by Asim et al., researchers fabricated an electrode material with properties of both SCs and lithium-ion batteries [31]. They achieved this by decorating CNT forests grown on carbon fiber substrates with RuO_2 nanorods (NRs) using chemical vapor deposition (CVD) followed by an annealing process. This design resulted in a material exhibiting a high C_{sp} (176 Fg^{-1}) and outstanding cycling stability, maintaining 97.0 % capacitance after 10,000 cycles at a current density (CD) of 40 mA cm^{-2} , as illustrated in Fig. 4.

Moreover, the material demonstrates a reversible areal capacity of 3.9 mAh cm^{-2} at 100 mA cm^{-2} in a lithium-ion battery electrode. This exceptional electrochemical performance stems from the synergistic interplay between the MO NRs and the architecture of the CNTS-CC. The expanded surface area and abundant active sites facilitated by this design enable efficient ingress and egress of ions and electrolytes within the electrode. Zhu et al. investigated a ternary NC composed of single-

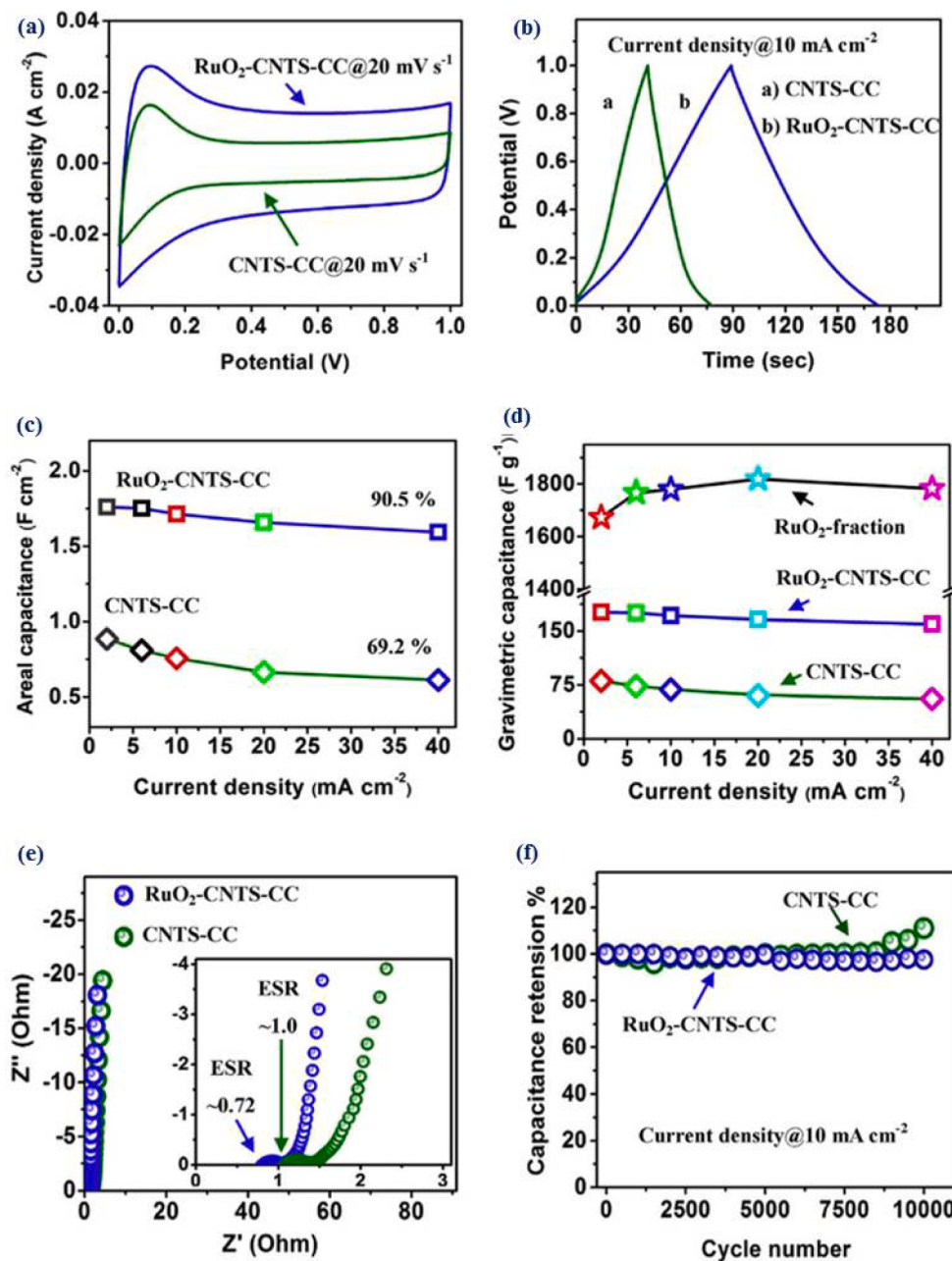


Fig. 4. Electrochemical Performance of Electrodes: (a) CV comparison, (b) GCD curves, (c) areal capacitance, (d) gravimetric capacitance, (e) Nyquist plots, (f) cyclic stability. Reproduced from Ref. [31]. [Copyright with permission from Elsevier, 2024].

walled CNT (SWCNTs), RuO₂, and polyindole (PIn) [32]. This material exhibited a remarkable C_{sp} of 1283 F g⁻¹ at a CD of 1.0 A g⁻¹. Furthermore, when employed in a symmetric SC, the SWCNT/RuO₂/PIn electrode delivered ED of 42 Wh kg⁻¹ and 33 Wh kg⁻¹ at PD of 500 W kg⁻¹ and 5000 W kg⁻¹, respectively. It displayed impressive cycling stability, maintaining a high capacitance of 1203 F g⁻¹ at 1.0 A g⁻¹. In a separate study, researchers synthesized CuCo₂O₄/CuO nanoneedles directly onto conductive Ni Foam via a hydrothermal and heat treatment process [33]. RuO₂ nanoparticles (NPs) were then deposited onto these nanoneedles. Beyond its application in SCs, CuCo₂O₄/CuO@RuO₂ demonstrates promising performance as a water oxidation catalyst. Notably, it exhibits a low overpotential (279.0 mV at 10.0 mA cm⁻²) and a favorable Tafel slope, indicating its efficiency in driving this reaction. Additionally, it boasts remarkable long-term stability. When employed in SCs, CuCo₂O₄/CuO@RuO₂ delivers an impressive areal capacity of up to 863 mAh cm⁻² and retains approximately 90.1 % of this capacity after

8,000 cycles, highlighting its excellent cycling stability. Furthermore, a hybrid SC constructed with CuCo₂O₄/CuO at RuO₂ and activated carbon (AC) achieves an ED of 0.84 mWh cm⁻² at a PD of 8 mW cm⁻².

Ates and Yildirim synthesized RuO₂-PANI and rGO/RuO₂-PANI NCs, achieving C_{sp} of 40F g⁻¹ and 723F g⁻¹, respectively [1]. Building upon these findings, Zhang et al. further optimized a PANI/RuO₂ electrode, reporting a superior C_{sp} of 816F g⁻¹ [34]. Cho et al. demonstrated exceptional performance with RuO₂ nanoneedles grown on a Ta/Cu current collector. This electrode exhibited a superior C_{sp} of 1420.0 F g⁻¹ at a low scan rate of 5.0 mV s⁻¹ and impressive cycling stability, retaining nearly 98.0 % of its capacitance even at a higher scan rate of 100.0 mV s⁻¹ after extended cycling. The electrode delivered an ED of 13.0 Wh kg⁻¹ at a PD of 27.0 kW kg⁻¹ [35]. Deshmukh et al. investigated PANI-RuO² composite thin films fabricated through a chemical bath deposition (CBD) method [36]. These films achieved a remarkable maximum C_{sp} of 830F g⁻¹, alongside impressive ED and PD of 216 Wh

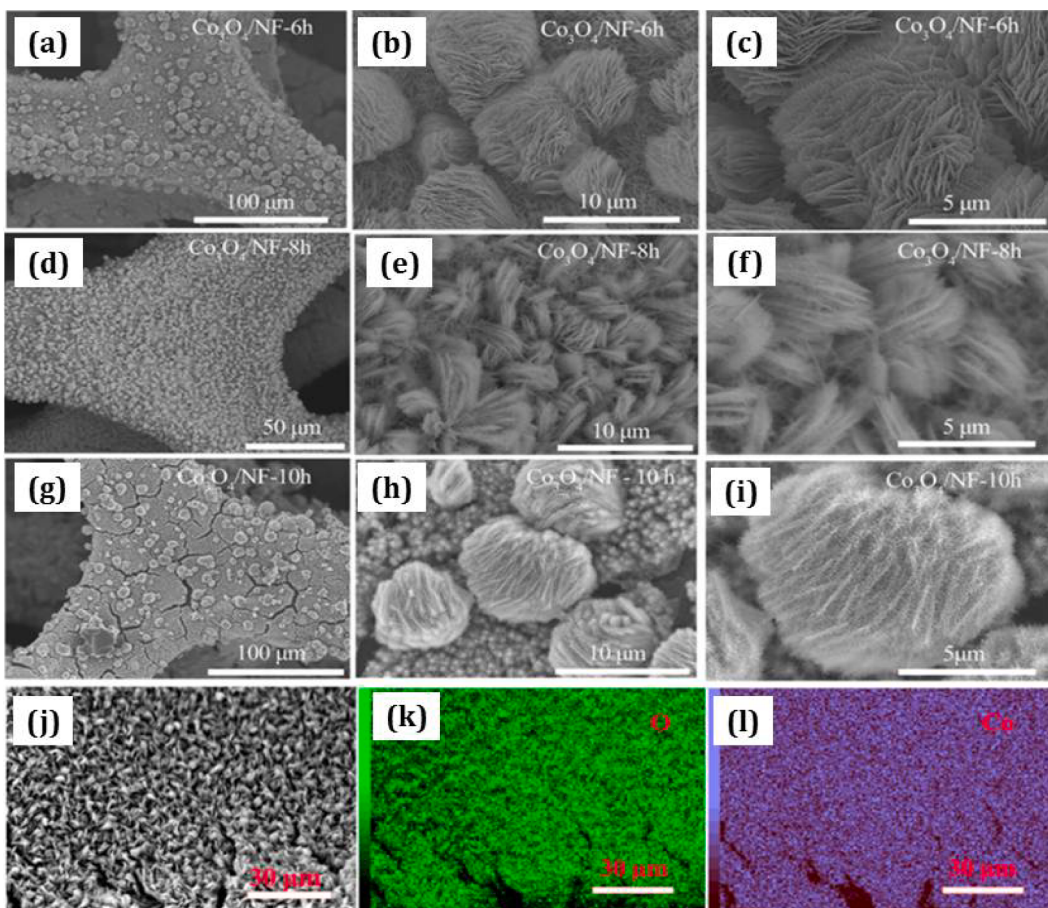


Fig. 5. SEM images: (a–c) Co_3O_4 -Ni foam for 6 hrs; (d–f) Co_3O_4 -NF for 8 hrs; (g–i) Co_3O_4 -NF for 10 hrs; (j–l) element mapping images of Co_3O_4 nanoflakes. Reproduced from Ref. [60]. [copyright with permission from Elsevier, 2024].

kg^{-1} and 4.2 kW kg^{-1} , respectively. Notably, the SILAR-synthesized composite delivered a C_{sp} of 664.0 F g^{-1} [37]. However, this SILAR-derived composite exhibited excellent cycling stability and retained approximately 89 % of its initial capacitance after 5,000 cycles. Thakur and Lokhande fabricated RuO²-incorporated PPy hybrid flexible electrodes, achieving a high C_{sp} of 1010.4 F g^{-1} at a low scan rate of 5 mV s^{-1} in $0.2 \text{ M Na}_2\text{SO}_4$ electrolyte [38]. Similarly, Liu et al. synthesized composite RuO₂/PEDOT nanotubes exhibiting a remarkable C_{sp} of 1217.0 F g^{-1} [39]. These nanotubes demonstrated exceptional PD, reaching 20 kW kg^{-1} , while maintaining 80 % of their maximum ED (28 Wh kg^{-1}).

2.2. Cobalt oxide (Co_3O_4)

Co_3O_4 , a TMO belonging to the spinel crystallographic family, exhibits faradaic redox reactions [51]. The following equation describes this process [40]:



Co_3O_4 emerges as a compelling candidate for SC electrodes due to its confluence of attractive properties: exceptional theoretical C_{sp} (3560 F g^{-1}), cost-effectiveness, environmental compatibility, and robust chemical stability [40–43,45]. However, a significant disparity exists between the theoretically predicted and experimentally observed capacitance in practical applications. This performance gap can be attributed to limitations in electron transport arising from inherently low conductivity, sluggish reaction kinetics, and substantial volume

expansion/contraction during charge-discharge cycling. Additionally, a propensity for particle aggregation further hinders the practical performance of Co_3O_4 [31,32,48,49].

- Co_3O_4 – based composite electrodes

Nanomaterials offer significant advantages for SC electrodes because of their inherently higher surface area, which translates to a large number of electrocatalytic sites [50]. The diminutive size of nanomaterials shortens the diffusion path for both electrons and ions, facilitating efficient charge transport within the electrode [44]. Recognizing the crucial role that material dimensionality and morphology play in enhancing electrochemical performance, a significant focus of research is on developing synthetic materials at the micro and nanoscale levels [46]. In pursuit of enhanced SC performance, a diverse array of Co_3O_4 nano-morphologies have been investigated, including Nanowires (NWs), nanofibers (NFs), NPs, and nanosheets [34–38]. A noteworthy approach involves the one-step hydrothermal and calcination method employed by Yue et al. for the preparation of Co_3O_4 /reduced graphene oxide (rGO) composites [52]. This environmentally benign method facilitates the formation of a three-dimensional structure featuring well-dispersed Co_3O_4 NPs anchored onto rGO flakes. The resulting Co_3O_4 /rGO-120-12 electrode capitalizes on this architecture to offer a significantly greater number of active sites compared to Co_3O_4 NWs [53]. This translates to superior electrochemical performance, as evidenced by the high C_{sp} of 1152 F g^{-1} achieved at a CD of 1 A g^{-1} .

In a seminal study, researchers led by I. Priyadharsini employed a sol-gel technique to synthesize Co_3O_4 NPs [54]. These NPs were subsequently incorporated into a composite electrode formulation with

carbon and polyvinylidene fluoride (PVDF) in an 8.0:1.0:1.0 mass ratio. The slurry was applied onto a Ni foam current collector. While the fabricated electrode exhibited a C_{sp} of 761.25 F g^{-1} at a CD of 11 mA cm^{-2} , the inclusion of PVDF presented a performance bottleneck. PVDF is known to elevate the interfacial resistance within the electrode-electrolyte interface, consequently diminishing the number of accessible active sites and hindering electron transport efficiency [55]. An alternative strategy involves the direct growth of Co_3O_4 onto conductive substrates such as carbon fibers, cloths, or metal foams. This approach eliminates the requirement for binders and conductive additives, potentially leading to enhanced SC performance [56].

Doping Co_3O_4 nanosheets grown directly on Ni foam with silver (Ag) significantly enhances their specific surface area [57]. Compared to pristine Co_3O_4 ($108 \text{ m}^2/\text{g}$), Ag-doped Co_3O_4 exhibits a remarkably high surface area of $176 \text{ m}^2 \text{ g}^{-1}$. This translates to outstanding rate capability, evident by the material retaining 92.84 % of its initial C_{sp} (1323 F g^{-1}) at a higher CD of 10 A g^{-1} . Additionally, the material demonstrates impressive cycling stability, exhibiting 105 % of its starting capacitance after 2000 cycles. For comparison, previously reported electrode materials by Yang et al. [58] and Wang et al. [59] delivered good electrochemical performances with C_{sp} of 883.0 F g^{-1} and 1606 F g^{-1} at a CD of 1 A g^{-1} , respectively. Wei et al. [60] presented electrodes with unique nanoarray structures. SEM micrographs of Co_3O_4 /Ni foam prepared with varying heating times are presented in Fig. 5 (a-i). Furthermore, elemental mapping images of the Co_3O_4 nanoflakes are illustrated in Fig. 5 (j-l).

The incorporation of Co_3O_4 NWs anchored onto the Co_3O_4 nanosheets significantly expands the surface area of the electrode. This expanded surface provides a wealth of active sites for Faradaic redox reactions, while also optimizing electrolyte ion conductivity. The sample synthesized via hydrothermally heating for 8 h ($\text{Co}_3\text{O}_4/\text{NF-8 hrs}$) exhibits a remarkable C_{sp} of 2053.1 F g^{-1} at a CD of 1 A g^{-1} . Furthermore, when integrated into an SC device with graphene, this heterostructure Co_3O_4 array allows for a working voltage of 1.6 V. The device delivers a maximum ED of 22.2 Wh kg^{-1} and demonstrates excellent cycling stability, retaining 93.3 % of its capacitance after 10,000 cycles.

Employing a heterogeneous precipitation technique, Wang et al. [61] synthesized a 3D structured Co_3O_4 network, achieving a remarkable C_{sp} of 820 F g^{-1} at a low scan rate of 5.0 mV s^{-1} . This electrode material boasts excellent durability, maintaining 90.2 % of its capacitance even after 1000 cycles. In a separate study, Liu et al. [62] prepared 1D Co_3O_4 NRs via hydrothermal methods. These NRs displayed a capacitance of 655 F g^{-1} at a CD of 0.5 A g^{-1} . The superior performance of the NRs is likely due to their high crystallinity and unique rod-like morphology [63]. Furthermore, Liu et al. investigated core-shell mesoporous Co_3O_4 nanospheres prepared using a solvothermal method. These core-shell structures delivered a capacitance of 837.7 F g^{-1} at 1.0 A g^{-1} and demonstrated impressive cycling durability, retaining 87 % of their capacitance after 2000 cycles at a higher CD of 5.0 A g^{-1} . Studies have attributed the high capacitance observed in core-shell mesoporous Co_3O_4 structures to their unique morphology [61]. This advantage is echoed in $\text{Co}_3\text{O}_4@\text{CoS}$ composites, where a core-shell architecture delivers an impressive C_{sp} of 1658 F g^{-1} at a CD of 1.0 A g^{-1} and exhibits excellent cycling stability, retaining 92 % of its capacitance after 10,000 cycles [64]. XRD analysis confirms the cubic lattice of Co_3O_4 , while the absence of a detectable CoS phase is likely owing to its reduced content within the core-shell material. The well-established synergy between carbonaceous materials and improved conductivity is further reinforced by the work of Naveen et al. [65]. Their synthesis of Co_3O_4 spinel structures on graphene nanospheres yielded a material with a C_{sp} of 650 F g^{-1} at a low scan rate of 5.0 mV s^{-1} and exceptional cycling durability, retained 92.0 % of its capacitance after 1000 cycles. Similarly, the advances of binary-oxide electrodes composed of crystalline NiCo_2O_4 composites on AC demonstrate promise for enhanced capacitance and conductivity. This improvement can be attributed to the presence of multiple redox couples, namely $\text{Co}^{2+}/\text{Co}^{3+}$ and $\text{Ni}^{3+}/\text{Ni}^{2+}$

[66]. Building upon the foundation of binary TMO electrodes, Xu et al. [66] explored composite electrodes, achieving a C_{sp} of 273.5 F g^{-1} at a CD of 1 A g^{-1} in a 6 mol/L KOH electrolyte. Notably, these electrodes exhibited exceptional cycling durability and retained 96.0 % of their capacitance after 3,000 cycles. This work underscores the significant influence of electrode morphology on electrochemical performance. Further investigations into the impact of mesoporous structure on Co_3O_4 were conducted by Qiu et al. [67]. The authors adopted a thermal-decomposition approach to facilitate the targeted growth of mesoporous nanocrystalline Co_3O_4 directly onto rGO nanosheets. This composite material delivered a remarkable C_{sp} of 1085.6 F g^{-1} at a high CD of 2.0 A g^{-1} in 2 mol L^{-1} KOH electrolyte, while maintaining impressive cycling stability with 83 % capacitance retention after 10,000 cycles. Obodo et al. [68] adopted a hydrothermal synthesis approach to create crystalline Co_3O_4 and MnO_2 NPs (approximately 30.0 nm crystallite size) supported on GO ($\text{Co}_3\text{O}_4\text{-MnO}_2$ at GO). This composite exhibited a unique, flake-like morphology. The resulting electrodes achieved a C_{sp} of 1518 F g^{-1} at a low scan rate of 10.0 mV s^{-1} in 1 mol L^{-1} Na_2SO_4 electrolyte.

Ren et al. [69] achieved impressive results with hierarchically hollow $\text{Co}_3\text{O}_4\text{-PANI}$ NC nanocages. These nanocages exhibited a remarkable C_{sp} of 1301 F g^{-1} at a CD of 1 A g^{-1} , along with a high ED of 41.5 Wh kg^{-1} at a PD of 0.8 kW kg^{-1} . Additionally, the nanocages demonstrated outstanding PD, reaching 15.8 kW kg^{-1} at 18 Wh kg^{-1} . Notably, these $\text{Co}_3\text{O}_4\text{/PANI}$ NCs displayed exceptional cycling stability, retaining 90 % of their capacitance after 2000 cycles. Zhenyin et al. [70] investigated core-shell PANI- Co_3O_4 NCs, achieving a C_{sp} of 1184 F g^{-1} at a CD of 1.25 A g^{-1} . These composites also exhibited high cycling stability and retained 84.9 % of their capacitance after 1000 cycles. Lin et al. [71] explored the potential of porous graphene/PANI/ Co_3O_4 (GPC) aerogels. This material displayed a high C_{sp} of 1247.0 F g^{-1} at a CD of 1.0 A g^{-1} and delivered outstanding durability, maintaining its capacitance throughout 3500 cycles. Guo et al. [52] fabricated hierarchical $\text{Co}_3\text{O}_4@\text{PPy}$ core-shell composite NWs exhibiting a remarkable C_{sp} of 2122 F g^{-1} at a low CD of 5.0 mA cm^{-2} . Additionally, these NWs displayed impressive cycling stability, retaining 77.8 % of their capacitance after 5000 cycles at a higher CD of 25 mA cm^{-2} . In a separate study, Sulaiman et al. [72] prepared a PEDOT/GO/ Co_3O_4 NC. This material demonstrated a C_{sp} of 535.60 F g^{-1} and excellent cycling durability, retaining 92.69 % of its capacitance after 2000 cycles. Yang et al. [73] focused on $\text{Co}_3\text{O}_4\text{/PEDOT}$ SCs. Their work yielded a material with a high areal capacitance of 160.0 mF cm^{-2} at a low CD of 0.2 mA cm^{-2} . Notably, this composite exhibited exceptional cycling stability and retained 93 % of its capacitance after 20,000 cycles.

2.3. Manganese oxide (MnO_2)

MnO_2 has garnered significant research interest as a potential SC electrode material due to its several attractive features [47,88]. These include its abundance in nature, minimal environmental impact, and exceptional theoretical C_{sp} of 1380 F g^{-1} [74,75,76]. However, a key challenge hindering its practical application lies in its inherently poor electrical conductivity and sluggish ion transport rate [64,65,66].

- Carbon Materials@ MnO_2 Composite Electrode

Due to their exceptional conductivity, stability, and high surface area, carbonaceous materials such as CNTs, graphene, and CNFs are demonstrably well-suited as scaffolds for MnO_2 nanostructure deposition [67,68]. These scaffolds offer a significant enhancement in active surface area and provide a multitude of active sites for electrochemical reactions [78,79]. Additionally, the presence of these carbonaceous materials shortens the diffusion pathway for electrolytes within the composite electrode, ultimately leading to improved electrochemical performance [80–82]. Cai et al. [83] successfully synthesized a 3-D core-shell composite electrode comprised of hollow N-doped carbon

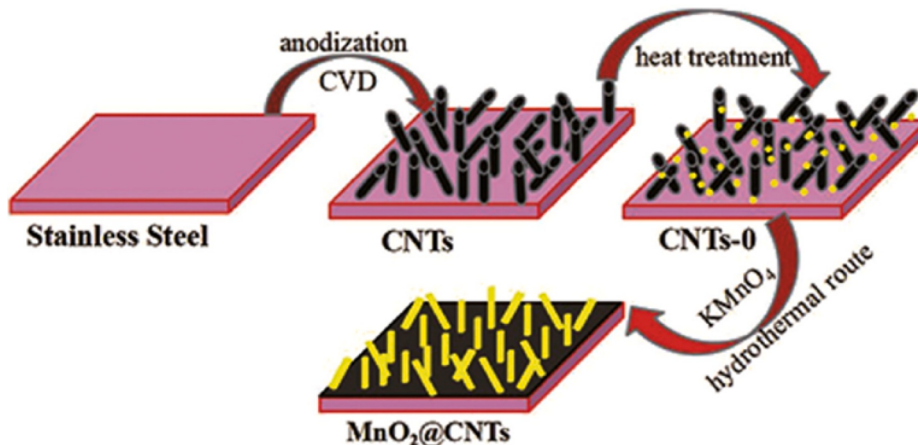


Fig. 6. Graphical representation of the core–shell MnO_2 at CNTs composite electrode prepared on a stainless steel substrate. Reproduced from Ref. [85]. [Copyright with permission from Elsevier, 2024].

(HNC) and MnO_2 . This composite exhibited a noteworthy electrochemical capacity of 247.9 F g^{-1} at a CD of 0.5 A g^{-1} . Furthermore, it displayed impressive capacity retention of 82.9 % at a significantly higher CD of 5 A g^{-1} after 2000 cycles. Highlighting the versatility of this approach, Long et al. [84] employed a simple one-step water bath process at 40°C to fabricate a flexible electrode. This electrode consisted of interconnected $\alpha\text{-MnO}_2$ nanosheets grown on AC cloth. The resulting electrode demonstrated remarkable charge storage performance with minimal degradation observed even after undergoing 2000 folding cycles. Notably, the asymmetric SC fabricated using this electrode achieved an ED of 49.8 Wh kg^{-1} at a PD of 1198.4 W kg^{-1} and maintained a remarkable capacitance retained 90.6 % after 5000 cycles. Another noteworthy example comes from the work of Lei et al. [85]. These researchers synthesized MnO_2 nanosheets grown on a network of graphitized CNTs (MnO_2 nanosheets @graphenated CNTs). This composite material was prepared on a 316 L stainless steel substrate using a combination of CVD and subsequent annealing treatment, as detailed in Fig. 6.

Graphenated CNTs are strategically linked to form a porous structure, providing an efficient pathway for electron transport. MnO_2 NPs are then uniformly distributed on this conductive scaffold. This unique architecture of MnO_2 nanosheets grown on graphenated CNTs offers several advantages: shortened ion diffusion paths, enhanced charge transfer kinetics, and accelerated reversible redox reactions. These factors collectively contribute to improved capacitance performance. Notably, this design achieves a high ED of 51.2 Wh kg^{-1} at 24.42 Wh cm^{-2} and a maximum PD of 0.4 kW kg^{-1} (200 W cm^2). For comparison, previous research by [86] employed a combined CVD and hydrothermal method to prepare a 3D graphene/ MnO_2 foam composite. Although lacking conductive carbon black additives, this composite electrode still exhibited a high C_{sp} of 333 F g^{-1} at 0.20 A g^{-1} .

Despite their desirable properties, the high cost and complex production processes associated with commercial carbon materials hinder large-scale applications. To address this challenge, research and development efforts are increasingly focused on low-cost and renewable alternatives. Biomass resources, with their high natural abundance and renewability, have emerged as a promising solution [87]. Biomass-derived carbon offers several advantages over traditional carbon materials, including eco-friendly materials, versatile structures, extended lifespan, and cost-effective production [17,76,77]. Additionally, the inherent stability and multistage pore structure of biomass carbon make it particularly well-suited for use in electrochemical materials. These qualities highlight the significant potential of biomass-derived carbon for SC applications. As an example, Yang et al. [91] successfully employed banana peels as a carbon source to synthesize MnO_2 /biomass-based porous carbon composites via a hydrothermal method. This

composite electrode exhibited a remarkable C_{sp} of 139.6 F g^{-1} at a CD of 300 mA g^{-1} and maintained a capacitance of 70 F g^{-1} even at a significantly higher CD of 10 A g^{-1} . Furthermore, the electrode displayed excellent cycling durability and retained over 92.0 % of its starting capacitance after 1000 cycles.

Shen et al. [92] explored the use of soybean pods as a precursor for the carbon matrix in MnO_2 /soybean pod carbon composites. Employing the hydrothermal method, they successfully synthesized a composite material that retained the tubular structure of the pods while incorporating a significant number of $\alpha\text{-MnO}_2$ NRs on its surface. Notably, the MnO_2/SPC electrode exhibited a superior C_{sp} (530 F g^{-1}) compared to the bare MnO_2 electrode (362 F g^{-1}). Furthermore, a symmetric SC fabricated using MnO_2/SPC electrodes demonstrated exceptional cycling stability, retaining 91 % of its capacitance after 6,000 cycles. This device exhibited ED of 35.1 Wh kg^{-1} at a high PD of 9000 W kg^{-1} , highlighting its potential for practical applications. Another study by [93] demonstrated the fabrication of hollow MnO_2 /carbon spheres (CSs) employing the hydrothermal method. This work highlights the versatility of biomass-derived carbon sources. Here, hollow carbon spheres were employed as a starting material, showcasing the potential of utilizing various biomass components. The resulting MnO_2 /hollow CS composite exhibited a hollow structure, likely contributing to its electrochemical performance. An asymmetric SC was assembled using this MnO_2 /hollow CS material as the positive electrode and the hollow CS alone as the negative electrode. This device achieved a maximum ED of 41.4 Wh kg^{-1} at a PD of 500 W kg^{-1} within a 2.0 V voltage window. It displayed impressive cycling durability, retaining 93.8 % after 5,000 cycles.

Zhao and Wang [94] accomplished a C_{sp} of 497 F g^{-1} with their MnO_2/PANI composites. This composite material also demonstrated impressive cycling stability, retaining 88.2 % of its capacitance after 5,000 cycles at a CD of 10.0 A g^{-1} . Liu et al. [95] focused on ternary hierarchical NFs comprised of $\text{MnO}_2/\text{PANI}/\text{MWCNT}$. This composite exhibited a capacitance of 348.5 F g^{-1} at a CD of 1 A g^{-1} and maintained cycling stability (88.2 % retention after 2,000 cycles). An asymmetric SC fabricated by Grover et al. [96] employed a coaxial MWCNT/PANI structure with MnO_2 as the positive electrode. This device achieved a C_{sp} of 324 F g^{-1} at a scan rate of 2.0 mA cm^{-2} and exhibited capacitance retention of 78 % after 3000 cycles at 3.0 mA cm^{-2} . Li et al. [97] investigated carbon cloth/ MnO_2/PANI NFs, achieving an even higher capacitance of 728.7 F g^{-1} at 1 A g^{-1} while demonstrating good cycling stability (87 % retention after 2,000 cycles). Pan et al. [98] explored PANI@ MnO_2 /graphene composites, reporting a remarkable C_{sp} of 695 F g^{-1} after 1000 cycles at a high CD of 4 A g^{-1} . Yin et al. [99], examined PEDOT-PSS/ MnO_2 hybrids, revealing a noteworthy C_{sp} of 366 F g^{-1} at a CD of 1 A g^{-1} . These hybrids accomplished capacitance retention after 2,000 cycles.

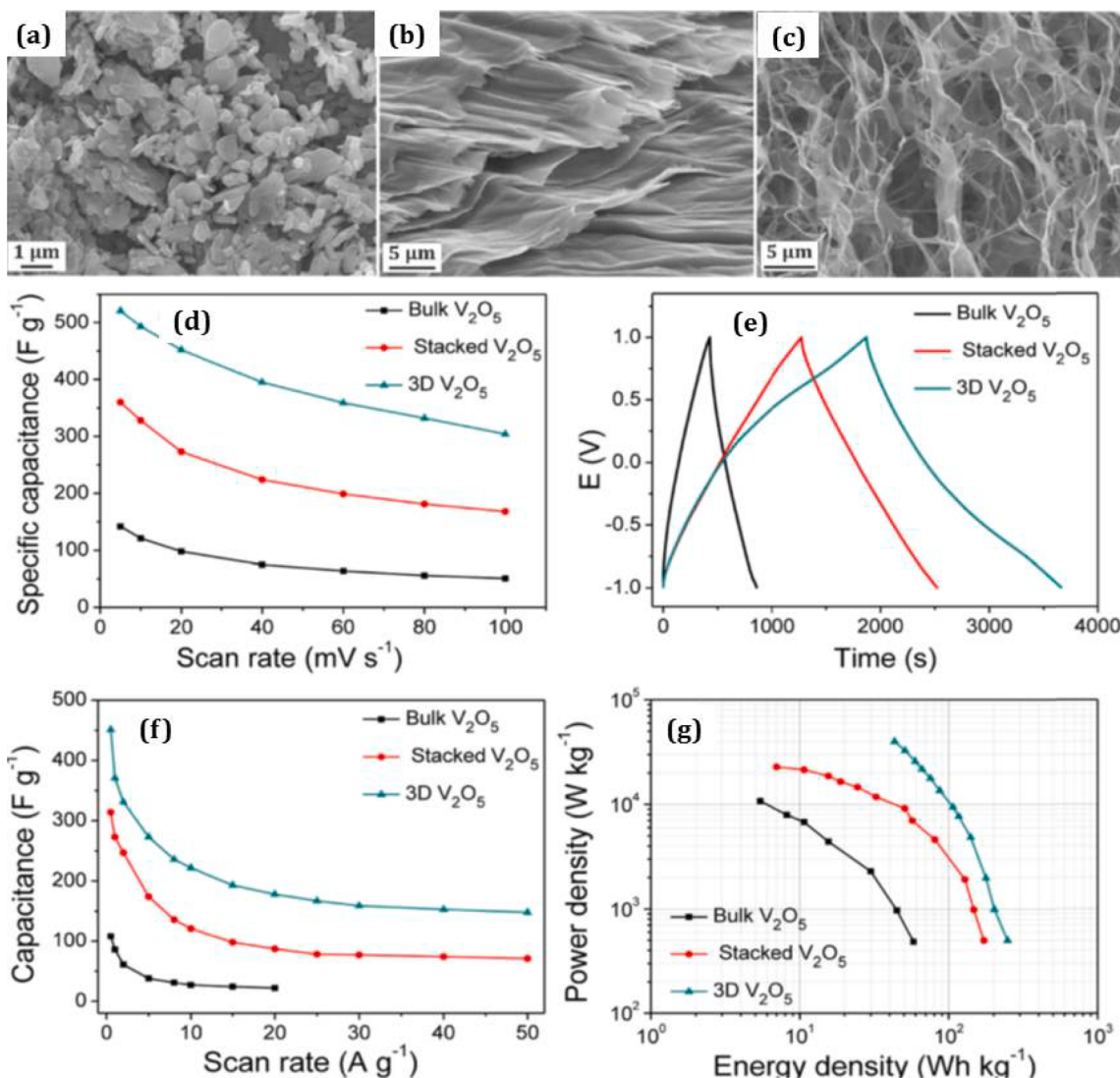


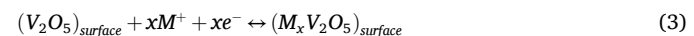
Fig. 7. FESEM images: (a) commercially available bulk, (b) staked films, and (c) 3D architecture constructed from. Electrochemical performance of 3D V_2O_5 , staked films, and bulk for SCs: (d) CV curves, (e) GCD curves, (f) rate capability Graphs; and (g) Regon Plots. Reproduced from Ref. [109]. [Copyright with permission from American Chemical Society, 2024].

2.4. Vanadium oxide (V_2O_5)

V_2O_5 has garnered considerable interest as a material for SC electrodes because of their physicochemical properties [104,105]. These properties include multiple oxidation states, exceptional chemical stability, and a wide potential window, all of which contribute to enhanced energy storage capabilities [100,102]. The pioneering work by Lee et al., enough demonstrated the viability of V_2O_5 for this application, achieving a C_{sp} of 350 F g^{-1} in an aqueous KCl electrolyte [100]. The development of nanostructured V_2O_5 has further propelled its potential for SC electrodes. Under their high surface-to-volume ratio, these nanostructures offer significantly increased electrolyte accessibility, ultimately improving charge storage efficiency. Wee et al. successfully employed electrospinning to fabricate V_2O_5 NFs [100]. These NFs accomplished a respectable SC of 190 F g^{-1} and ED of 5 Wh kg^{-1} in a 2 M KCl electrolyte. Notably, even greater performance was observed in a Li-ion-containing organic electrolyte, where the V_2O_5 NFs delivered an SC of 250 F g^{-1} and a remarkable ED of 78 Wh kg^{-1} [100]. These findings highlight the potential of nanostructured V_2O_5 for achieving superior energy storage performance in SCs.

V_2O_5 exhibits a rich variety of oxidation states, ranging from 0 to +5, leading to the formation of compounds like VO_2 , V_2O_3 , and itself

[101]. V_2O_5 can be reduced to VO_2 (oxidation state +5 to +4) depending on certain environmental factors like temperature, pressure, and acidity/basicity [89,90]. Notably, V_2O_5 has extensively investigated vanadium oxide and finds application for application in Li-ion, Na-ion, and Mg-ion battery electrodes due to its favorable properties [91,92]. Beyond batteries, V_2O_5 holds significant promise for SCs owing to its high C_{sp} and cost-effectiveness. The orthorhombic phase of V_2O_5 is a strong candidate for energy storage due to superior ion storage. Additionally, V_2O_5 boasts conductivity and superior stability among vanadium oxides, with a melting temperature of $685.0 \text{ }^\circ\text{C}$ [103]. The pseudocapacitive behavior of V_2O_5 arises from intercalation processes occurring within its crystal structure. These processes involve the reversible insertion and removal of ions, leading to morphological and surface chemistry changes as depicted reaction below [106]:



V_2O_5 exhibits exceptional promise as a SC electrode material due to its unique structural characteristics. The presence of both two-dimensional (2D) layered morphology and a complex three-dimensional (3D) architecture with interconnected channels facilitates efficient electrolyte ion diffusion throughout the electrode [107]. This optimized ionic accessibility is paramount for maximizing the rate

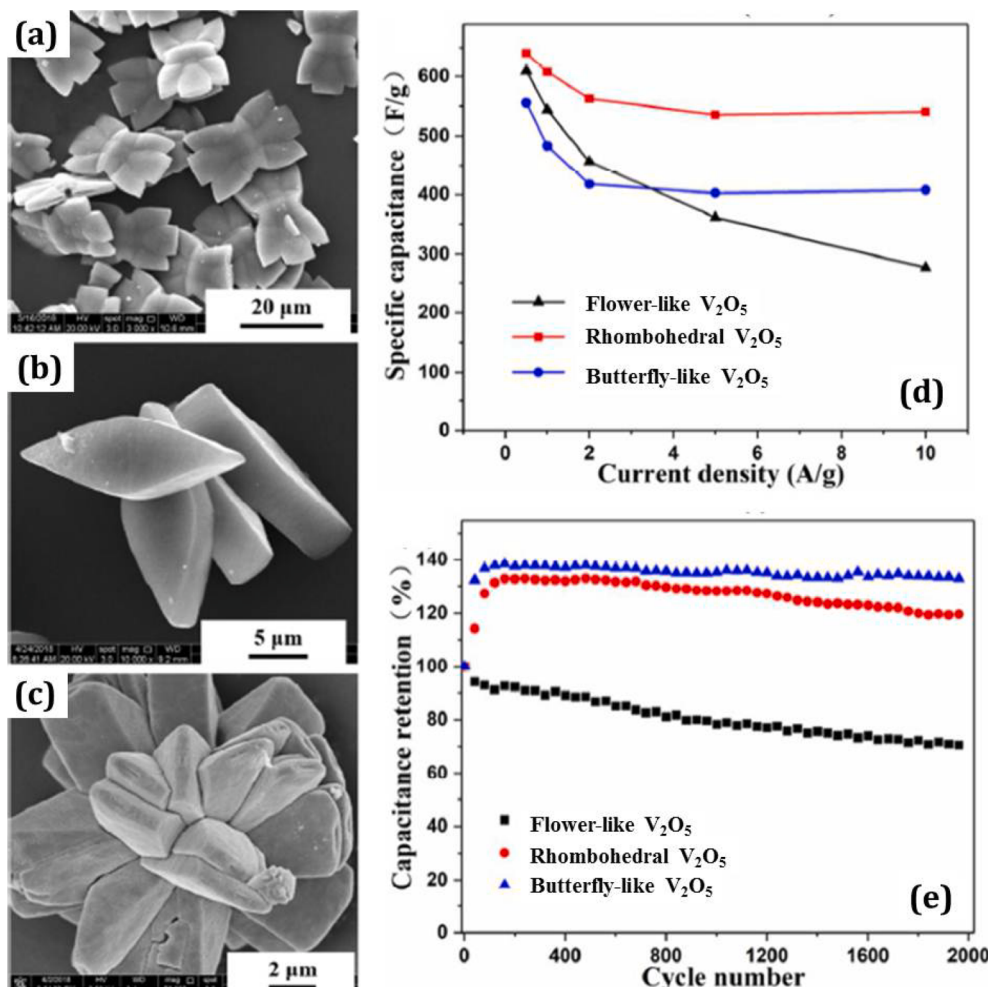


Fig. 8. SEM micrographs of (a) butterfly-shaped, (b) rhombohedral, (e) flower-shaped V₂O₅. Electrochemical performance: (d) C_{sp} vs CD graph; and (e) CV curves [112]. [copyright with permission from American Chemical Society, 2024].

Reproduced from Ref. [112]

capability of the material during charge and discharge cycles. Furthermore, V₂O₅ demonstrates remarkable structural stability in diverse electrolytes, including both aqueous and organic media. This characteristic allows for the utilization of a broad potential window during operation[107]. A wider potential window directly translates to enhanced ED in the resulting SC device. Theoretical calculations predict a maximum capacitance of 883F g⁻¹ for a single V₂O₅ monolayer, assuming participation in the ion adsorption process as outlined in reaction (3) within a 1.2 V potential range [108]. However, real-world capacitances typically fall below this value due to limitations in fully utilizing the theoretical surface area of the electrode material. In contrast to ion adsorption, intercalation processes also contribute to the overall capacitance of V₂O₅ electrodes. However, these processes are highly dependent on the porosity and overall morphological structure of the material.

Zhu et al. [109] investigated the influence of V₂O₅ crystal NP morphology on electrochemical performance. They compared three distinct morphologies: bulk, stacked, and 3D structures (Fig. 7 (a-c)). Notably, the complex 3D structure exhibited superior electrochemical efficiency, characterized by higher C_{sp}, PD, and ED. This enhanced performance can be attributed to the significantly larger surface area (approximately 133 m² g⁻¹) of the 3D structure compared to the other morphologies. X-ray diffraction analysis revealed distinct crystallinity between the structures. The bulk sample displayed a crystalline phase with well-defined peaks corresponding to various crystal planes [(001), (003), (004), (005), (006), and (007)]. Conversely, the 3D structure

exhibited a more limited set of peaks, with preferential orientation along the (001) plane. This preferential orientation, along with the formation of channels by interconnected 2D V₂O₅ sheets, is believed to contribute to the higher surface area observed in the 3D morphology. The optimized structure facilitated efficient electrolyte ion diffusion, leading to a remarkable capacitance of 451F g⁻¹ at a CD of 0.50 A g⁻¹ in a Na₂SO₄ (1 M) electrolyte. This capacitance significantly surpasses the values achieved by stacked V₂O₅ (314.0F g⁻¹) and bulk V₂O₅ (108.0F g⁻¹), highlighting the advantages of the 3D architecture for SC applications shown in Fig. 7 (d-g) [109].

This study investigates the effect of crystal structure and, morphology on the performance of V₂O₅ as an SC electrode material. Generally, amorphous oxides exhibit lower energy losses compared to their crystalline counterparts due to the presence of channels that facilitate ionic diffusion [110]. In the case of V₂O₅, achieving optimal capacitance is highly reliant on its morphology. Qian et al. [111] explored the formation of V₂O₅ in various crystalline morphologies, including NWs, and flower-shaped flakes. While one-dimensional (1D) V₂O₅ NWs demonstrated a high initial capacitance (349F g⁻¹) attributable to their large surface area (123 m²/g), their capacitance retention was significantly compromised, dropping to 27.6 % after only 200 charge-discharge cycles. Conversely, hydrated V₂O₅ curly bundled NWs exhibited an increase in capacitance (from 42.0 to 127.0F g⁻¹) after cycling, potentially enabled by nanopores within their structure [111]. Building upon this work, Zheng et al. [112] synthesized V₂O₅ microstructures with distinct morphologies: butterfly-shaped, rhombohedral,

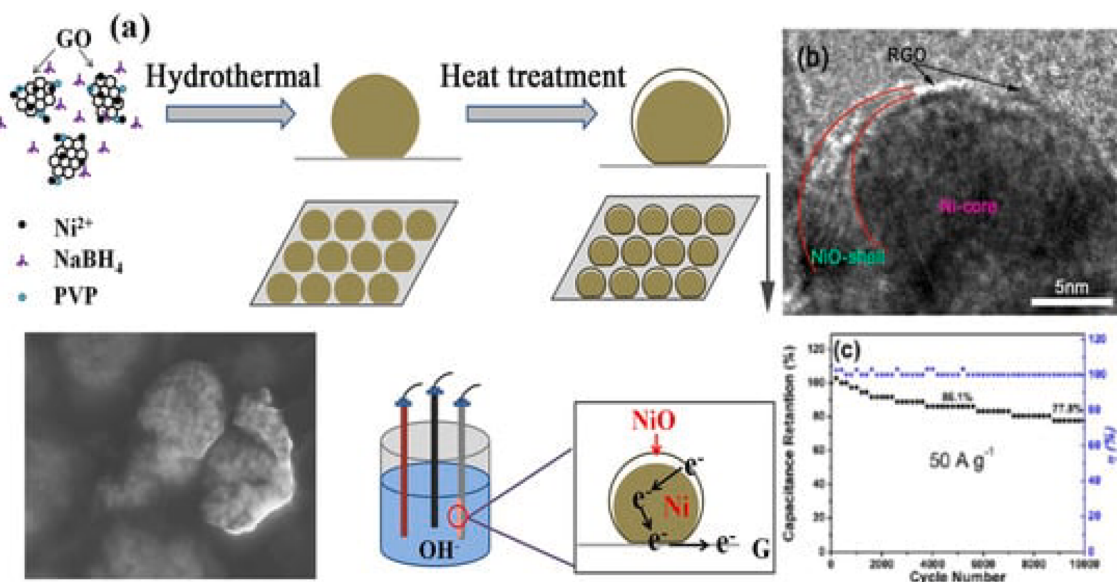


Fig. 9. (a) Schematic depicting the conductive mechanism within the material. (b) HR-TEM images of the NiO/Ni/RGO; (c) Columbia efficiency of the electrode [121].

and flower-shaped. These microstructures displayed remarkable capacitances of 556, 641, and 609F g⁻¹, respectively, at a CD of 0.5 A g⁻¹ in a 1.0 molL⁻¹ LiClO₄ electrolyte (Fig. 8 (a-d)). Notably, all these microstructures were crystalline V₂O₅, but with an orthorhombic crystal structure. The performance of the rhombohedral structure was linked to its simplistic morphology, which promotes efficient surface polarization even at low electrolyte concentrations. In contrast, butterflies as well as flower-shaped structures required high electrolyte concentrations to promote pronounced polarization. Furthermore, electrochemical impedance spectroscopy revealed a lower electrical resistivity for the rhombohedral structure (0.76 Ω) compared to the butterfly-like (1.22 Ω) and flower-like (1.17 Ω) structures. This indicates faster ionic diffusion within the rhombohedral structure, contributing to its higher capacitance. The rhombohedral structure also demonstrated exceptional capacitance retention (119.8 % after 2,000 cycles) compared to the butterfly-like (132.6 %) and flower-like (70.4 %) structures (Fig. 8 (e)). The observed capacitance enhancement during cycling can likely be attributed to the inherent material porosity [112]. These findings highlight the critical role of crystal structure and morphology in optimizing the electrochemical performance of V₂O₅ for SC applications.

Bai et al. [113] developed V₂O₅/PANI composites NWs achieving a high C_{sp} and excellent stability. They reported superior ED and PD, along with capacitance retention exceeding 90 % after numerous charge-discharge cycles. Asen et al. [114] investigated a V₂O₅/PPy/GO NC demonstrating exceptional C_{sp} at high CD. This composite delivered impressive ED and PD while maintaining good cyclic stability over thousands of cycles. Bi et al. [115] fabricated G- V₂O₅/PEDOT nanocable-based SCs exhibiting remarkable C_{sp} and ED in a neutral electrolyte. Notably, these SCs displayed outstanding cycling life, retaining over 120 % of their starting capacitance after 50,000 cycles. These studies highlight the potential of V₂O₅ composites for SC applications, delivering exceptional performance with high capacitance, fast charging, and long-lasting stability.

2.5. Nickel oxide (NiO)

NiO has garnered significant interest in recent research because of its wide range of physicochemical characteristics encompassing thermal, photoconductive, electrical, acoustic, catalytic, and magnetic functionalities [7]. Notably, NiO boasts both environmental compatibility and abundant natural reserves, making it a strategic material for various

applications. SCs represent a particularly promising area where NiO demonstrates exceptional theoretical potential.

A key advantage of NiO for SC electrodes lies in its ability to exhibit multiple oxidation states. This characteristic facilitates rapid redox reactions, which are crucial for efficient energy storage mechanisms [116]. Theoretical calculations predict a remarkable capacitance of 2585F g⁻¹ for NiO at a potential window of 0.50 V. In contrast, this value remains elusive in practice due to intrinsically NiO exhibits conductivity values between 0.010 and 0.320 S/m [117]. This limitation hinders the efficient utilization of the material, resulting in a significant gap between theoretical and experimentally achieved capacitances. Additionally, NiO exhibits volume expansion/contraction during charge/discharge processes, potentially leading to the degradation of active materials and disruption of electrical pathways within the electrode structure [118]. Consequently, experimentally measured C_{sp} for NiO electrodes, even those incorporating nanostructures and high surface area (SSA), typically range from 50 to 1776F g⁻¹ [119].

The exact mechanism by which NiO-based electrodes store energy remains a topic of ongoing investigation. Two primary hypotheses attempt to explain the relationship between NiO and its hydrated form, nickel oxyhydroxide (NiOOH). One model posits that energy storage occurs via reversible conversion between NiO and NiOOH during electrochemical processes [108]. Conversely, the other hypothesis suggests an initial transformation of NiO to nickel hydroxide (Ni(OH)₂) under alkaline conditions. This is followed by further interactions in Ni(OH)₂ and the electrolyte to generate NiOOH [120]. Further research is necessary to definitively identify the dominant mechanism governing energy storage in NiO electrodes.



The incorporation of graphene (Gr) facilitates the formation of Ni/NiO core-shell architecture with partial NiO coverage, as shown in Fig. 9. This unique architecture leads to an exceptional C_{sp} of 2048.3F g⁻¹ at a CD of 1 A g⁻¹. Moreover, the composite electrode accomplishes remarkable cyclic stability, retaining 77.8 % after 10,000 cycles at 50 A g⁻¹ [121].

Singu et al. [122] reported PANI-NiO NCs with a C_{sp} of 514 Fg⁻¹ at a scan rate of 1.0 mV/s. Zhang et al. [123] further improved upon this performance by fabricating ACNF/PANI/NiO ternary composites,

Table 1

TMOs for SC electrode.

Sr. No	Material	Synthesis / Preparation Technique	Electrolyte	C_{sp} (Fg $^{-1}$)	Reference
1	RuO ₂	Sol-gel	0.5 M H ₂ SO ₄	720	[127]
2	RuO ₂	Electrodeposition	1.0 M H ₂ SO ₄	788	[128]
3	RuO ₂	Electrodeposition	0.5 M H ₂ SO ₄	650	[129]
4	RuO ₂ -TiO ₂	Chemical	1.0 M KOH	46	[130]
5	RuO ₂ -SnO ₂	Sol-gel	1.0 M H ₂ SO ₄	690	[131]
6	RuO ₂ -C	Colloidal	1.0 M H ₂ SO ₄	407	[132]
7	RuO ₂ -C composite	Colloidal solution	1.0 M H ₂ SO ₄	250	[133]
8	Ni(OH) ₂	CBD	2.0 M KOH	398	[134]
9	NiO	CBD	2.0 M KOH	167	[135]
10	Ni(OH) ₂	SILAR	2.0 M KOH	350	[136]
11	NiO _x	Electrodeposition	1.0 M KOH	277	[137]
12	NiO-RuO ₂	Co-precipitation	1.0 M KOH	210	[138]
13	mesoporous NiO	Sol-gel	1.0 M KOH	125	[139]
14	Ni-Co	CVD	1.0 M KOH	569	[140]
15	Ni(OH) ₂	Electrodeposition	3.0 M KOH	578	[141]
16	NiO	Calcination	2.0 M KOH	120	[142]
17	Co ₃ O ₄	Template-free growth method	6.0 M KOH	746	[143]
18	Co ₃ O ₄	SILAR	1.0 M KOH	165	[144]
19	RuO ₂	Templating	1.0 M H ₂ SO ₄	954	[145]
20	Co-MnO ₂	Electrodeposition	0.5 M Na ₂ SO ₄	396	[146]
21	Co-MnO ₂	Electrodeposition	1.0 M Na ₂ SO ₄	498	[147]
22	Co ₃ O ₄	Spray pyrolysis	2.0 M KOH	74	[148]
23	V ₂ O ₅	Chemical method	0.1 M H ₂ SO ₄	170	[13]
24	IrO ₂ -MnO ₂	Thermal decomposition	0.5 M H ₂ SO ₄	550	[149]
25	Nano MnO ₂	Soft chemical route	1.0 M Na ₂ SO ₄	211	[150]
26	NiO-AC NC	Co-precipitation	6.0 M KOH	84.8	[151]
27	ZnO-AC NC	Co-precipitation	6.0 M KOH	341.6	[152]
			1.0 M NaOH	335.3	
28	Mn ₂ O ₃ -Mn ₃ O ₄ -AC NC	Co-precipitation	1.0 M H ₂ SO ₄	305.6	[153]
			6.0 M KOH	187.8	
29	RuO ₂	Hydrothermal	1.0 M H ₂ SO ₄	400	[24]
30	NiO	Electrochemical precipitation	1.0 M KOH	146	[154]
31	MnO ₂ nanosheets/hollow CNFs	hydrothermal	1.0 M Na ₂ SO ₄	293.6	[75]
32	CeO ₂ /Co ₃ O ₄ /rGO NPs	hydrothermal	6.0 M KOH	1606.6	[59]
33	RuO ₂	Electrophoretic deposition	1.0 M H ₂ SO ₄	734	[10]
34	ZnO nanomembranes	atomic layer deposition	6.0 M KOH	846	[155]
35	Co ₃ O ₄ -CuO-ZnO/GO	hydrothermal	0.5 M Na ₂ SO ₄	2045	[156]
36	ZnO@rGO	Direct microwave irradiation	0.1 M KOH	102.4	[157]
37	RuO ₂	Spray pyrolysis	0.5 M H ₂ SO ₄	551	[158]
38	PANI/MnO ₂	—	1.0 M H ₂ SO ₄	417	[159]
39	PANI/NiO//SGO	—	6.0 M KOH	308.8	[160]
40	PANI/Co ₃ O ₄ //AC	—	6.0 M KOH	3105.46	[161]
41	PANI/ Co ₃ O ₄ //ZIF-8NPC	—	KOH	1407	[162]
42	PPy / MnO ₂ // C ₃ N ₄	—	1.0 M aqueous Na ₂ SO ₄	509.4	[163]
43	PPy/V ₂ O ₅ // f-CNT	—	1.0 M Na ₂ SO ₄	1266 mF cm $^{-2}$	[164]
44	PPy/ZnO	—	1.0 M KCl	161.02	[165]
45	PPy/NiO//CoO	—	2.0 M KOH	1123	[166]
46	PEDOT/ MnO ₂ //NCC	—	1.0 M KCL	144.69	[167]
47	PEDOT/V ₂ O ₅ //Graphene	—	5.0 M LiCl	22.4 mF cm $^{-2}$	[168]
48	PEDOT/Co ₃ O ₄ //CNFs	—	—	849.65	[169]
49	CuCo ₂ O ₄ /CuO@RuO ₂	—	2.0 M KOH	862.5 mAh cm $^{-2}$	[33]
50	Co ₃ O ₄ @MnO ₂ on carbon cloth	—	1.0 M Na ₂ SO ₄	616.7	[170]
51	ZnO/CeO ₂	—	3.0 M KOH	495.4	[171]
52	RuO ₂ //h-WO ₃	—	—	47.59	[172]
53	Co3O4//AC	—	—	310.4	[53]
54	Co ₃ O ₄ -NF-8h//N-rGO/NF	—	—	62.5	[60]
55	MnO ₂ /HCS-30//HCS	—	—	74.5	[93]
56	NiCo ₂ O ₄ @MnO ₂ /AC	—	—	112	[173]
57	RuO ₂ -carbon	Electroless deposition	H ₂ SO ₄	190	[174]
58	RuO ₂	Colloidal method	H ₂ SO ₄	863	[132]
59	RuO ₂ /SnO ₂ xerogel	Incipient wetness method	KOH	710	[175]
60	AC/RuO ₂	Sol-gel	H ₂ SO ₄	1340	[176]
61	RuO ₂	Anodic deposition	H ₂ SO ₄	740	[177]
62	RuO ₂ /Graphene	Disassembly-reassembly strategy	H ₂ SO ₄	1485	[178]
63	MnO ₂	Electro deposition	Na ₂ SO ₄	698	[179]
64	α -MnO ₂	Co-precipitation	Na ₂ SO ₄	166	[180]
65	α -MnO ₂	Hydrothermal	Na ₂ SO ₄	168	[181]
66	α -MnO ₂	Micro emulsion	Na ₂ SO ₄	297	[182]
67	MnO ₂	Potentiodynamic	Na ₂ SO ₄	392	[183]
68	NiO	Hydrothermal	—	390	[184]
69	NiO	Electroless plating	—	586.4	[185]
70	NiO	CBD	—	309	[186]

(continued on next page)

Table 1 (continued)

Sr. No	Material	Synthesis / Preparation Technique	Electrolyte	C_{sp} (Fg ⁻¹)	Reference
71	NiO	Thermal oxidation	—	1784.2	[187]
72	Co ₃ O ₄ @NiO	Hydrothermal	—	91.3	[188]
73	ZnO@C@NiO	CBD, Hydrothermal	—	677	[189]
74	NiO/Graphene	SIMILAR	—	783	[190]
75	Ni(OH) ₂	CBD	—	1065	[191]
76	MnO ₂ -Ni.(OH) ₂	Hydrothermal	—	1015	[192]
77	Co ₃ O ₄ @Ni.(OH) ₂	Hydrothermal	—	1306	[193]
78	ZnS/ZnO/Ni(OH) ₂	Hydrothermal	—	1773	[194]
79	MnO ₂ /C	—	0.5 M Na ₂ SO ₄	258	[195]
80	PANI/MnO ₂ /FC	—	1.0 M H ₂ SO ₄	289	[196]
81	WO ₃ -V ₂ O ₅	—	6.0 M KOH	173	[197]
82	Co ₃ O ₄ /Ni	—	6.0 M KOH	1,060	[198]

achieving a superior C_{sp} of 1157 Fg⁻¹ and demonstrating excellent cycling durability, retaining 93.8 % of its capacitance after 5,000 cycles. Cho et al. [124] demonstrated NiO and PANI-PSS NCs exhibiting capacitance of 834F/g at 1.0 Ag⁻¹ and higher capacitance retaining 88.9 % after 3,000 cycles. Yang et al. [125] investigated NiO and Ni(OH)₂/PEDOT hybrid electrodes, delivering C_{sp} of 404.1 mF cm⁻¹ at 4 mA cm⁻¹ and higher cycling life retention of 82 % after 1,000 cycles. Notably, Han et al. [126] reported exceptional performance with their NiO/PPy-6 composite electrodes. These electrodes achieved a remarkable C_{sp} of 3648.6 Fg⁻¹ at 3.0 A g⁻¹ and maintained a capacitance of 1784F g⁻¹ at 30 A g⁻¹. The device made with NiO/PPy-6 and AC delivered a remarkable capacitance of 938 Fg⁻¹ at 3.0 A/g, a good ED of 333 Whkg⁻¹, and an impressive PD of 2399.9 Wkg⁻¹.

A comprehensive overview of the most commonly utilized TMOs for SC electrode fabrication can be found in Table 1.

3. Unique properties of MO-based NCs

MO-based NCs exhibit a compelling synergy between MOs and incorporated materials like graphene, CNTs, and polymers. This synergistic interaction unlocks a remarkable array of properties leading to demonstrably superior electrochemical performance in SC devices.

Crucially, the integration of highly conductive nanomaterials like graphene and CNTs fosters enhanced electrical conductivity within the NC. This translates to efficient charge transfer kinetics, minimizing resistance and enabling rapid charge-discharge cycles. Furthermore, the high surface area offered by these nanomaterials translates to a dramatic increase in the electrode-electrolyte interface. This expanded area allows for the storage of a greater number of ions, ultimately resulting in superior C_{sp} values.

Beyond these benefits, MO-based NCs offer the advantage of precisely controlled porosity and pore size distribution due to the incorporation of nanomaterials. This engineered pore structure optimizes ion diffusion and electrolyte accessibility, leading to improved charge storage capabilities. Additionally, the combination of pseudocapacitance from MOs and double-layer capacitance of conductive nanomaterials creates a synergistic charge storage mechanism. This enables the NC to exploit both chemical reactions (faradaic) and physical interactions (non-faradaic) for efficient energy storage, yielding superior ED. Notably, the incorporation of graphene and CNTs also enhances the mechanical stability of MO-based NCs. These conductive nanomaterials help to mitigate volume expansion issues during cycling, thereby preventing structural degradation and extending the cycle life of SC electrodes.

The unique properties of MO-based NCs empower the design of SCs with exceptional performance metrics. These tailored characteristics can be precisely engineered to meet the specific energy storage requirements of various applications. From enabling rapid energy delivery to facilitating the development of flexible and lightweight designs for wearable electronics, MO-based NCs represent a transformative force in the future of SC technology.

4. Challenges and future prospective

The incorporation of MO-based NCs as advanced SC electrode materials offers significant promise. However, several key challenges require focused attention. A critical one is material stability. While some MOs, like ruthenium oxide, exhibit exceptional electrochemical performance, their long-term cyclability and ability to withstand repeated charge-discharge cycles remain a concern. Mitigating material degradation and developing robust, long-lasting SCs are paramount for future research efforts. Scalability presents another hurdle. Many advanced synthesis techniques for these NCs are currently restricted to the laboratory environment. To fully realize their potential for practical applications, research into scalable manufacturing processes that can address the growing demand for energy storage solutions is crucial. Finally, cost considerations and environmental impact are critical aspects that cannot be ignored. Identifying cost-effective alternatives and developing environmentally friendly production processes are essential for promoting widespread adoption and ensuring sustainability technology.

Advanced characterization can guide the design of high-performance SC materials. Research into novel MOs, nanomaterials, and multifunctional composites offers promise for achieving exceptional electrochemical performance. A critical focus lies in bridging the gap between fundamental research and practical applications. The translation of fundamental research into tangible societal benefits hinges on the successful integration of these novel materials EVs, portable electronics, and renewable energy storage. Sustainability remains paramount. Developing environmentally friendly NCs alongside material recycling and reuse strategies aligns perfectly with the global pursuit of sustainable energy solutions. Overcoming current limitations and exploring these promising research avenues are critical to unlocking the transformative potential of MO-based NCs for next-generation SC applications.

5. Conclusion

In conclusion, this review dives deep into SC technology, emphasizing the paramount role of electrode materials in determining their electrochemical performance. SCs are emerging as a highly attractive option for energy storage applications owing to their superior PD and fast charge-discharge characteristics. However, optimizing their efficiency hinges on the strategic selection of suitable electrode materials. Several MOs, particularly MnO₂, NiO, RuO₂, Co₃O₄, and V₂O₅ have garnered considerable research interest due to their attractive redox properties and electrochemical activity. This review has specifically highlighted a transformative approach – the integration of MO-based NCs with materials like graphene, CNT, and polymers. This synergistic combination offers compelling advantages: enhanced electrical conductivity, expanded surface area, and amplified charge storage capabilities. These advancements have the potential to revolutionize SC technology. As the need for high-performance and environmentally responsible energy storage solutions becomes increasingly critical, the

exploration of novel materials like MO-based NCs paves the way for significant breakthroughs in this field. This review underscores the unwavering commitment of the scientific community to advancing energy storage technologies, ultimately contributing to a more sustainable and electrified future.

CRediT authorship contribution statement

Dadaso D Mohite: Writing – original draft, Software, Methodology, Investigation. **Sachin S Chavan:** Validation, Supervision, Conceptualization. **Prasad E Lokhande:** Writing – review & editing, Supervision, Methodology. **Kailasnath B Sutar:** Writing – review & editing, Supervision, Data curation. **Sumit Dubal:** Supervision, Methodology. **Udaybhaskar Rednam:** Visualization, Formal analysis, Data curation. **Bandar Ali Al-Asbahi:** Visualization, Data curation. **Yedluri Anil Kumar:** Visualization, Data curation.

Declaration of competing interest

The authors declare that they have no known competing financial interests or personal relationships that could have appeared to influence the work reported in this paper.

Data availability

No data was used for the research described in the article.

Acknowledgment

The authors extend their thanks to Researchers Supporting Project Number (RSP2024R348), King Saud University, Riyadh, Saudi Arabia.

References

- [1] M. Ates, M. Yildirim, The synthesis of rGO/RuO₂, rGO/PANI, RuO₂/PANI and rGO/RuO₂/PANI nanocomposites and their supercapacitors, *Polym. Bull.* 77 (5) (May 2020) 2285–2307, <https://doi.org/10.1007/s00289-019-02850-8>.
- [2] P.E. Lokhande, U.S. Chavan, A. Pandey, Materials and Fabrication Methods for Electrochemical Supercapacitors: Overview, *Electrochem. Energy Rev.* 3 (1) (Mar. 2020) 155–186, <https://doi.org/10.1007/s41918-019-00057-z>.
- [3] D.D. Mohite, S.S. Chavan, S. Dubal, P.B. Karandikar, Electrosyn polycrylonitrile (PAN) carbon nanofibers (CFNs) as electrode material for supercapacitors: A comprehensive review of synthesis, characterization, and electrochemical performance, *AIP Adv.* 13 (12) (Dec. 2023) 120703, <https://doi.org/10.1063/5.0177740>.
- [4] N. Lakal, S. Dubal, P.E. Lokhande, “Supercapacitors: An introduction”, in *Nanotechnology in the Automotive Industry*, Elsevier (2022) 459–466, <https://doi.org/10.1016/B978-0-323-90524-4.00022-0>.
- [5] S. Parida, et al., High performance supercapacitor electrodes from automobile soots: An effective approach to control environmental pollution, *Inorg. Chem. Commun.* 158 (Dec. 2023) 111671, <https://doi.org/10.1016/j.inoche.2023.111671>.
- [6] Y. Ma, et al., Recent advances in transition metal oxides with different dimensions as electrodes for high-performance supercapacitors, *Adv. Compos. Hybrid Mater.* 4 (4) (Dec. 2021) 906–924, <https://doi.org/10.1007/s42114-021-00358-2>.
- [7] R.S. Keth, S.A. Khalate, R.J. Deokate, Overview of nanostructured metal oxides and pure nickel oxide (NiO) electrodes for supercapacitors: A review, *J. Alloys Compd.* 734 (Feb. 2018) 89–111, <https://doi.org/10.1016/j.jallcom.2017.10.262>.
- [8] L. Zhang, A. Aboagye, A. Kelkar, C. Lai, H. Fong, A review: carbon nanofibers from electrosyn polycrylonitrile and their applications, *J. Mater. Sci.* 49 (2) (Jan. 2014) 463–480, <https://doi.org/10.1007/s10853-013-7705-y>.
- [9] A. Afif, S. M. Rahman, A. Tasfiah Azad, J. Zaini, M. A. Islam, and A. K. Azad, “Advanced materials and technologies for hybrid supercapacitors for energy storage – A review,” *J. Energy Storage*, vol. 25, p. 100852, Oct. 2019, doi: 10.1016/j.est.2019.100852.
- [10] M.S. Yadav, Metal oxides nanostructure-based electrode materials for supercapacitor application, *J. Nanoparticle Res.* 22 (12) (Dec. 2020) 367, <https://doi.org/10.1007/s11051-020-05103-2>.
- [11] D.D. Mohite, V. Chaturvedi, S. De, V.S. Jadhav, *Nanomaterials in Automotive Applications: A Review and its Technical Aspects*, *Int. J. Contemp. Archit. New ARCH* 8 (2) (2021) 1450–1460.
- [12] B.B. Sahoo, et al., A state-of-art review on 2D material-boosted metal oxide nanoparticle electrodes: Supercapacitor applications, *J. Energy Storage* 65 (Aug. 2023) 107335, <https://doi.org/10.1016/j.est.2023.107335>.
- [13] T. Cottineau, M. Toupin, T. Delahaye, T. Brousse, D. Bélanger, Nanostructured transition metal oxides for aqueous hybrid electrochemical supercapacitors, *Appl. Phys. A* 82 (4) (Mar. 2006) 599–606, <https://doi.org/10.1007/s00339-005-3401-3>.
- [14] Y.V. Thorat, S.S. Chavan, D.D. Mohite, Electro spun PAN Nanofiber with Optimized Diameter, *Journal of Algebraic Statistics* 13 (2) (2022) 1447–1454, <https://doi.org/10.52783/jas.v13i2.309>.
- [15] M. A. A. Mohd Abdah, N. H. N. Azman, S. Kulandaivalu, and Y. Sulaiman, “Review of the use of transition-metal-oxide and conducting polymer-based fibres for high-performance supercapacitors,” *Mater. Des.*, vol. 186, p. 108199, Jan. 2020, doi: 10.1016/j.matdes.2019.108199.
- [16] V. Ruhela, M.I. Ansari, P.V. Jadhav, D.D. Mohite, M.J. Patil, P.A. Dixit, A. Harale, An experimental investigation of photo chemical machining process for stainless-steel material by using different etchants, *Materials Today: Proceedings* (2023), <https://doi.org/10.1016/j.matpr.2023.03.324>.
- [17] N. S. George, L. Maria Jose, and A. Aravind, “Review on Transition Metal Oxides and Their Composites for Energy Storage Application,” in *Updates on Supercapacitors*, Z. Stevic, Ed., IntechOpen, 2023. doi: 10.5772/intechopen.108781.
- [18] U.S. Pawar, S.S. Chavan, D.D. Mohite, Synthesis of glass FRP-natural fiber hybrid composites (NFHC) and its mechanical characterization, *Discov. Sustain.* 5 (1) (Mar. 2024) 44, <https://doi.org/10.1007/s43621-024-00231-4>.
- [19] D.D. Mohite, A. Goyal, A.S. Singh, M.I. Ansari, K.A. Patil, P.D. Yadav, P. V. Londhe, Improvement of thermal performance through nanofluids in industrial applications: A review on technical aspects, *Materials Today: Proceedings* (2023), <https://doi.org/10.1016/j.matpr.2024.04.083>.
- [20] B.B. Sahoo, V.S. Pandey, A.S. Dogonchi, D.N. Thatoi, N. Nayak, M.K. Nayak, Synthesis, characterization and electrochemical aspects of graphene based advanced supercapacitor electrodes, *Fuel* 345 (Aug. 2023) 128174, <https://doi.org/10.1016/j.fuel.2023.128174>.
- [21] D. D. Mohite *et al.*, “Mechanism for segregation of cutting fluid and scrap for industrial application,” *Mater. Today Proc.*, p. S2214785323012026, Mar. 2023, doi: 10.1016/j.matpr.2023.03.160.
- [22] B.B. Sahoo, V.S. Pandey, A.S. Dogonchi, D.N. Thatoi, N. Nayak, M.K. Nayak, Exploring the potential of borophene-based materials for improving energy storage in supercapacitors, *Inorg. Chem. Commun.* 154 (Aug. 2023) 110919, <https://doi.org/10.1016/j.inoche.2023.110919>.
- [23] D. D. Mohite, V. S. Jadhav, A. N. Nayak, and S. S. Chavan, “An influence of CNC grinding wheel dressing parameters on Ra value of EN19 steel,” *Mater. Today Proc.*, p. S2214785323008040, Mar. 2023, doi: 10.1016/j.matpr.2023.02.260.
- [24] F. Yu, L. Pang, H.-X. Wang, Preparation of mulberry-like RuO₂ electrode material for supercapacitors, *Rare Met.* 40 (2) (Feb. 2021) 440–447, <https://doi.org/10.1007/s12598-020-01561-8>.
- [25] Y. Xie, C. Yao, Electrochemical performance of RuO₂-TiO₂ nanotube hybrid electrode material, *Mater. Res. Express* 6 (12) (Jan. 2020) 125550, <https://doi.org/10.1088/2053-1591/ab69c9>.
- [26] C.-W. Kuo, J.-C. Chang, B.-W. Wu, T.-Y. Wu, Electrochemical characterization of RuO₂-Ta₂O₅/polyaniline composites as potential redox electrodes for supercapacitors and hydrogen evolution reaction, *Int. J. Hydrog. Energy* 45 (42) (Aug. 2020) 22223–22231, <https://doi.org/10.1016/j.ijhydene.2019.08.059>.
- [27] J. Xu, et al., Flexible Asymmetric Supercapacitors Based upon Co₉S₈ Nanorod//Co₃O₄@RuO₂ Nanosheet Arrays on Carbon Cloth, *ACS Nano* 7 (6) (Jun. 2013) 5453–5462, <https://doi.org/10.1021/nn401450s>.
- [28] M. Manuraj, J. Chacko, K. N. Narayanan Unni, and R. B. Rakhi, “Heterostructured MoS₂-RuO₂ nanocomposite: A promising electrode material for supercapacitors,” *J. Alloys Compd.*, vol. 836, p. 155420, Sep. 2020, doi: 10.1016/j.jallcom.2020.155420.
- [29] S. Park, et al., Combustion-driven synthesis route for tunable TiO₂/RuO₂ hybrid composites as high-performance electrode materials for supercapacitors, *Chem. Eng. J.* 384 (Mar. 2020) 123269, <https://doi.org/10.1016/j.cej.2019.123269>.
- [30] A.M. Patil, et al., Fabrication of three-dimensionally heterostructured rGO/WO₃-0.5H₂O@Cu₂S electrodes for high-energy solid-state pouch-type asymmetric supercapacitor, *Chem. Eng. J.* 403 (Jan. 2021) 126411, <https://doi.org/10.1016/j.cej.2020.126411>.
- [31] S. Asim, et al., RuO₂ nanorods decorated CNTs grown carbon cloth as a free standing electrode for supercapacitor and lithium ion batteries, *Electrochim. Acta* 326 (Dec. 2019) 135009, <https://doi.org/10.1016/j.electacta.2019.135009>.
- [32] D. Zhu, et al., Two-step preparation of carbon nanotubes/RuO₂/polyindole ternary nanocomposites and their application as high-performance supercapacitors, *Front. Mater. Sci.* 14 (2) (Jun. 2020) 109–119, <https://doi.org/10.1007/s11706-020-0497-5>.
- [33] P. Zhang, X. Liu, H. He, Y. Peng, Y. Wu, Engineering RuO₂ on CuCo₂O₄/CuO nanoneedles as multifunctional electrodes for the hybrid supercapacitors and water oxidation catalysis, *J. Alloys Compd.* 832 (Aug. 2020) 154962, <https://doi.org/10.1016/j.jallcom.2020.154962>.
- [34] G. Zhang, et al., Controllable Intercalated Polyaniline Nanofibers Highly Enhancing the Utilization of Delaminated RuO₂ Nanosheets for High-Performance Hybrid Supercapacitors, *ChemElectroChem* 9 (9) (May 2022) e202200039.
- [35] S. Cho, et al., Self-assembled RuO₂ nanoneedles on Ta/Cu foil for a robust and high-performance supercapacitor electrode, *Surf. Interfaces* 31 (Jul. 2022) 102069, <https://doi.org/10.1016/j.surfin.2022.102069>.
- [36] P.R. Deshmukh, R.N. Bulakhe, S.N. Pusawale, S.D. Sartale, C.D. Lokhande, Polyaniline-RuO₂ composite for high performance supercapacitors: chemical synthesis and properties, *RSC Adv.* 5 (36) (2015) 28687–28695, <https://doi.org/10.1039/C4RA16969G>.

- [37] P.R. Deshmukh, S.V. Patil, R.N. Bulakhe, S.D. Sartale, C.D. Lokhande, Inexpensive synthesis route of porous polyaniline-ruthenium oxide composite for supercapacitor application, *Chem. Eng. J.* 257 (Dec. 2014) 82–89, <https://doi.org/10.1016/j.cej.2014.06.038>.
- [38] A.V. Thakur, B.J. Lokhande, Study of RuO₂ incorporated PPY hybrid flexible electrodes prepared by soaking and drying technique: a novel approach, *Appl. Phys. A* 127 (12) (Dec. 2021) 910, <https://doi.org/10.1007/s00339-021-05028-0>.
- [39] R. Liu, J. Duay, T. Lane, S. Bok Lee, Synthesis and characterization of RuO₂/poly (3,4-ethylenedioxythiophene) composite nanotubes for supercapacitors, *Phys. Chem. Chem. Phys.* 12 (17) (2010) 4309, <https://doi.org/10.1039/b918589p>.
- [40] C. Zhang, et al., Hierarchically porous Co₃O₄/C nanowire arrays derived from a metal–organic framework for high performance supercapacitors and the oxygen evolution reaction, *J. Mater. Chem. A* 4 (42) (2016) 16516–16523, <https://doi.org/10.1039/C6TA06314D>.
- [41] S. Adhikari, S. Selvaraj, S. Ji, D. Kim, Encapsulation of Co₃O₄ Nanocone Arrays via Ultrathin NiO for Superior Performance Asymmetric Supercapacitors, *Small* 16 (48) (Dec. 2020) 2005414, <https://doi.org/10.1002/smll.202005414>.
- [42] X. Wang, et al., Preparation and Electrochemical Properties of Co₃O₄ Supercapacitor Electrode Materials, *Crystals* 10 (9) (Aug. 2020) 720, <https://doi.org/10.3390/cryst10090720>.
- [43] Q. Liao, N. Li, S. Jin, G. Yang, C. Wang, All-Solid-State Symmetric Supercapacitor Based on Co₃O₄ Nanoparticles on Vertically Aligned Graphene, *ACS Nano* 9 (5) (May 2015) 5310–5317, <https://doi.org/10.1021/acsnano.5b00821>.
- [44] X. Wang, S. Yin, J. Jiang, H. Xiao, X. Li, A tightly packed Co₃O₄/C@S composite for high-performance electrochemical supercapacitors from a cobalt(III) cluster-based coordination precursor, *J. Solid State Chem.* 288 (Aug. 2020) 121435, <https://doi.org/10.1016/j.jssc.2020.121435>.
- [45] J. Lu, et al., A facile strategy of in-situ anchoring of Co₃O₄ on N doped carbon cloth for an ultrahigh electrochemical performance, *Nano Res.* 14 (7) (Jul. 2021) 2410–2417, <https://doi.org/10.1007/s12274-019-3242-6>.
- [46] M. Chatterjee, S. Sain, A. Roy, S. Das, S.K. Pradhan, Enhanced electrochemical properties of Co₃O₄ with morphological hierarchy for energy storage application: A comparative study with different electrolytes, *J. Phys. Chem. Solids* 148 (Jan. 2021) 109733, <https://doi.org/10.1016/j.jpcs.2020.109733>.
- [47] J. Cao, et al., Tunable agglomeration of Co₃O₄ nanowires as the growing core for in-situ formation of Co₂NiO₄ assembled with polyaniline-derived carbonaceous fibers as the high-performance asymmetric supercapacitors, *J. Alloys Compd.* 853 (Feb. 2021) 157210, <https://doi.org/10.1016/j.jallcom.2020.157210>.
- [48] J. Deng, et al., Solution combustion synthesis of cobalt oxides (Co₃O₄ and Co₃O₄/CoO) nanoparticles as supercapacitor electrode materials, *Electrochim. Acta* 132 (Jun. 2014) 127–135, <https://doi.org/10.1016/j.electacta.2014.03.158>.
- [49] C. Xiang, M. Li, M. Zhi, A. Manivannan, N. Wu, A reduced graphene oxide/Co₃O₄ composite for supercapacitor electrode, *J. Power Sources* 226 (Mar. 2013) 65–70, <https://doi.org/10.1016/j.jpowsour.2012.10.064>.
- [50] R. Kumar, S.M. Youssry, H.M. Soe, M.M. Abdel-Galeil, G. Kawamura, A. Matsuda, Honeycomb-like open-edged reduced-graphene-oxide-enclosed transition metal oxides (NiO/Co₃O₄) as improved electrode materials for high-performance supercapacitor, *J. Energy Storage* 30 (Aug. 2020) 101539, <https://doi.org/10.1016/j.est.2020.101539>.
- [51] Z. Ji, et al., Nitrogen-doped carbon dots anchored NiO/Co₃O₄ ultrathin nanosheets as advanced cathodes for hybrid supercapacitors, *J. Colloid Interface Sci.* 579 (Nov. 2020) 282–289, <https://doi.org/10.1016/j.jcis.2020.06.070>.
- [52] X.-M. Yue, et al., Synthesis of Co₃O₄/reduced graphene oxide by one step-hydrothermal and calcination method for high-performance supercapacitors, *Ionics* 27 (1) (Jan. 2021) 339–349, <https://doi.org/10.1007/s11581-020-03797-x>.
- [53] Y. Zhao, H. Liu, P. Hu, J. Song, L. Xiao, Asymmetric hybrid capacitor based on Co₃O₄ nanowire electrode, *Ionics* 26 (12) (Dec. 2020) 6289–6295, <https://doi.org/10.1007/s11581-020-03695-2>.
- [54] C.I. Priyadharsini, et al., Sol-Gel synthesis of Co₃O₄ nanoparticles as an electrode material for supercapacitor applications, *J. Sol-Gel Sci. Technol.* 96 (2) (Nov. 2020) 416–422, <https://doi.org/10.1007/s10971-020-05393-x>.
- [55] C. Guan, X. Liu, W. Ren, X. Li, C. Cheng, J. Wang, Rational Design of Metal-Organic Framework Derived Hollow NiCo₂O₄ Arrays for Flexible Supercapacitor and Electrocatalysis, *Adv. Energy Mater.* 7 (12) (Jun. 2017) 1602391, <https://doi.org/10.1002/aenm.201602391>.
- [56] H. Chen, X. Du, J. Sun, R. Wu, Y. Wang, C. Xu, Template-free synthesis of novel Co₃O₄ micro-bundles assembled with flakes for high-performance hybrid supercapacitors, *Ceram. Int.* 47 (1) (Jan. 2021) 716–724, <https://doi.org/10.1016/j.ceramint.2020.08.181>.
- [57] M. Aadil, S. Zulfiqar, M. Shahid, S. Haider, I. Shakir, M.F. Warsi, Binder free mesoporous Ag-doped Co₃O₄ nanosheets with outstanding cyclic stability and rate capability for advanced supercapacitor applications, *J. Alloys Compd.* 844 (Dec. 2020) 156062, <https://doi.org/10.1016/j.jallcom.2020.156062>.
- [58] X. Yang, et al., Low-temperature synthesis of sea urchin-like Co-Ni oxide on graphene oxide for supercapacitor electrodes, *J. Mater. Sci. Technol.* 55 (Oct. 2020) 223–230, <https://doi.org/10.1016/j.jmst.2020.03.026>.
- [59] Z. Wang, K. Zhao, S. Lu, W. Xu, Application of flammulina-velutipes-like CeO₂/Co₃O₄/rGO in high-performance asymmetric supercapacitors, *Electrochim. Acta* 353 (Sep. 2020) 136599, <https://doi.org/10.1016/j.electacta.2020.136599>.
- [60] G. Wei, et al., The hetero-structured nanoarray construction of Co₃O₄ nanowires anchored on nanoflakes as a high-performance electrode for supercapacitors, *Appl. Surf. Sci.* 538 (Feb. 2021) 147932, <https://doi.org/10.1016/j.apsusc.2020.147932>.
- [61] Y. Wang, Y. Lei, J. Li, L. Gu, H. Yuan, D. Xiao, Synthesis of 3D-Nanonet Hollow Structured Co₃O₄ for High Capacity Supercapacitor, *ACS Appl. Mater. Interfaces* 6 (9) (May 2014) 6739–6747, <https://doi.org/10.1021/am500464n>.
- [62] Z. Liu, et al., Facile synthesis of homogeneous core-shell Co₃O₄ mesoporous nanospheres as high performance electrode materials for supercapacitor, *J. Alloys Compd.* 774 (Feb. 2019) 137–144, <https://doi.org/10.1016/j.jallcom.2018.09.347>.
- [63] V. Venkatachalam, A. Alsalmi, A. Alsweileh, R. Jayavel, Shape controlled synthesis of rod-like Co₃O₄ nanostructures as high-performance electrodes for supercapacitor applications, *J. Mater. Sci. Mater. Electron.* 29 (7) (Apr. 2018) 6059–6067, <https://doi.org/10.1007/s10854-018-8580-8>.
- [64] Y. Lu, et al., Room-temperature sulfurization for obtaining Co₃O₄/CoS core-shell nanosheets as supercapacitor electrodes, *J. Alloys Compd.* 818 (Mar. 2020) 152877, <https://doi.org/10.1016/j.jallcom.2019.152877>.
- [65] A.N. Naveen, P. Manimaran, S. Selladurai, Cobalt oxide (Co₃O₄)/graphene nanosheets (GNS) composite prepared by novel route for supercapacitor application, *J. Mater. Sci. Mater. Electron.* 26 (11) (Nov. 2015) 8988–9000, <https://doi.org/10.1007/s10854-015-3582-2>.
- [66] J. Xu, et al., Hydrothermal Synthesis of NiCo₂O₄ /Activated Carbon Composites for Supercapacitor with Enhanced Cycle Performance, *ChemistrySelect* 2 (18) (Jun. 2017) 5189–5195, <https://doi.org/10.1002/slct.201700777>.
- [67] D. Qiu, X. Ma, J. Zhang, B. Zhao, Z. Lin, In situ synthesis of mesoporous Co₃O₄ nanorods anchored on reduced graphene oxide nanosheets as supercapacitor electrodes, *Chem. Phys. Lett.* 710 (Oct. 2018) 188–192, <https://doi.org/10.1016/j.cplett.2018.08.082>.
- [68] R.M. Obodo, et al., Performance Evaluation of Graphene Oxide Based Co₃O₄@GO, MnO₂ @GO and Co₃O₄/MnO₂ @GO Electrodes for Supercapacitors, *Electroanalysis* 33 (12) (Dec. 2020) 2786–2794, <https://doi.org/10.1002/elan.202060262>.
- [69] X. Ren, H. Fan, J. Ma, C. Wang, M. Zhang, N. Zhao, Hierarchical Co₃O₄/PANI hollow nanocages: Synthesis and application for electrode materials of supercapacitors, *Appl. Surf. Sci.* 441 (May 2018) 194–203, <https://doi.org/10.1016/j.apsusc.2018.02.013>.
- [70] Z. Hai, et al., Facile synthesis of core-shell structured PANI-Co₃O₄ nanocomposites with superior electrochemical performance in supercapacitors, *Appl. Surf. Sci.* 361 (Jan. 2016) 57–62, <https://doi.org/10.1016/j.apsusc.2015.11.171>.
- [71] H. Lin, et al., Self-Assembled Graphene/Polyaniline/Co₃O₄ Ternary Hybrid Aerogels for Supercapacitors, *Electrochim. Acta* 191 (Feb. 2016) 444–451, <https://doi.org/10.1016/j.electacta.2015.12.143>.
- [72] Y. Sulaiman, M. K. S. Azmi, M. A. M. Abduh, and N. H. N. Azman, “One step electrodeposition of poly(3,4-ethylenedioxothiophene)/graphene oxide/cobalt oxide ternary nanocomposite for high performance supercapacitor,” *Electrochimica Acta*, vol. 253, pp. 581–588, Nov. 2017, doi: 10.1016/j.electacta.2017.09.103.
- [73] P. Yang, J. Xie, C. Guo, C.M. Li, Soft- to network hard-material for constructing both ion- and electron-conductive hierarchical porous structure to significantly boost energy density of a supercapacitor, *J. Colloid Interface Sci.* 485 (Jan. 2017) 137–143, <https://doi.org/10.1016/j.jcis.2016.06.060>.
- [74] Y. Huang, S. Bao, J. Lu, Flower-like MnO₂/polyaniline/hollow mesoporous silica as electrode for high-performance all-solid-state supercapacitors, *J. Alloys Compd.* 845 (Dec. 2020) 156192, <https://doi.org/10.1016/j.jallcom.2020.156192>.
- [75] J. Noh, C.-M. Yoon, Y.K. Kim, J. Jang, High performance asymmetric supercapacitor twisted from carbon fiber/MnO₂ and carbon fiber/MoO₃, *Carbon* 116 (May 2017) 470–478, <https://doi.org/10.1016/j.carbon.2017.02.033>.
- [76] S.D. Raut, et al., Electrochemically grown MnO₂ nanowires for supercapacitor and electrocatalysis applications, *New J. Chem.* 44 (41) (2020) 17864–17870, <https://doi.org/10.1039/DONJ03792C>.
- [77] W. Lu, Y. Li, M. Yang, X. Jiang, Y. Zhang, Y. Xing, Construction of Hierarchical Mn 203@MnO2 Core-Shell Nanofibers for Enhanced Performance Supercapacitor Electrodes, *ACS Appl. Energy Mater.* 3 (9) (Sep. 2020) 8190–8197, <https://doi.org/10.1021/acsma.0c00392>.
- [78] Janardhanan. R. Rani, R. Thangavel, M. Kim, Y. S. Lee, and J.-H. Jang, “Ultra-High Energy Density Hybrid Supercapacitors Using MnO2/Reduced Graphene Oxide Hybrid Nanoscrolls,” *Nanomaterials*, vol. 10, no. 10, p. 2049, Oct. 2020, doi: 10.3390/nano10102049.
- [79] P. Liu, et al., Rational construction of bowl-like MnO₂ nanosheets with excellent electrochemical performance for supercapacitor electrodes, *Chem. Eng. J.* 350 (Oct. 2018) 79–88, <https://doi.org/10.1016/j.cej.2018.05.169>.
- [80] B. Liu, et al., Optimized synthesis of nitrogen-doped carbon with extremely high surface area for adsorption and supercapacitor, *Appl. Surf. Sci.* 538 (Feb. 2021) 147961, <https://doi.org/10.1016/j.apsusc.2020.147961>.
- [81] B. Padhy, R. Kali, P.K. Enaganti, N. Narasaiah, P.K. Jain, Facile synthesis and frequency-response behavior of supercapacitor electrode based on surface-etched nanoscaled-graphene platelets, *Colloids Surf. Physicochem. Eng. Asp.* 609 (Jan. 2021) 125587, <https://doi.org/10.1016/j.colsurfa.2020.125587>.
- [82] P. Zhao, M. Yao, H. Ren, N. Wang, S. Komarneni, Nanocomposites of hierarchical ultrathin MnO₂ nanosheets/hollow carbon nanofibers for high-performance asymmetric supercapacitors, *Appl. Surf. Sci.* 463 (Jan. 2019) 931–938, <https://doi.org/10.1016/j.apsusc.2018.09.041>.
- [83] W. Cai, R.K. Kankala, M. Xiao, N. Zhang, X. Zhang, Three-dimensional hollow N-doped ZIF-8-derived carbon@MnO₂ composites for supercapacitors, *Appl. Surf. Sci.* 528 (Oct. 2020) 146921, <https://doi.org/10.1016/j.apsusc.2020.146921>.
- [84] X. Long, et al., Interconnected δ-MnO₂ nanosheets anchored on activated carbon cloth as flexible electrode for high-performance aqueous asymmetric

- supercapacitors, *J. Electroanal. Chem.* 877 (Nov. 2020) 114656, <https://doi.org/10.1016/j.jelechem.2020.114656>.
- [85] R. Lei, et al., Construction of MnO₂ nanosheets@graphenated carbon nanotube networks core-shell heterostructure on 316L stainless steel as binder-free supercapacitor electrodes, *Int. J. Hydrog. Energy* 45 (53) (Oct. 2020) 28930–28939, <https://doi.org/10.1016/j.ijhydene.2019.09.070>.
- [86] X.-L. Bai, et al., Supercapacitor performance of 3D-graphene/MnO₂ foam synthesized via the combination of chemical vapor deposition with hydrothermal method, *Appl. Phys. Lett.* 117 (18) (Nov. 2020) 183901, <https://doi.org/10.1063/5.0018708>.
- [87] C. Xiong, et al., Fabrication of eco-friendly carbon microtubes @ nitrogen-doped reduced graphene oxide hybrid as an excellent carbonaceous scaffold to load MnO₂ nanowall (PANI nanorod) as bifunctional material for high-performance supercapacitor and oxygen reduction reaction catalyst, *J. Power Sources* 447 (Jan. 2020) 227387, <https://doi.org/10.1016/j.jpowsour.2019.227387>.
- [88] C. Li, et al., MnO_x nanosheets anchored on a bio-derived porous carbon framework for high-performance asymmetric supercapacitors, *Appl. Surf. Sci.* 527 (Oct. 2020) 146842, <https://doi.org/10.1016/j.apsusc.2020.146842>.
- [89] M. Li, J. Yu, X. Wang, Z. Yang, 3D porous MnO₂@carbon nanosheet synthesized from rambutan peel for high-performing supercapacitor electrodes materials, *Appl. Surf. Sci.* 530 (Nov. 2020) 147230, <https://doi.org/10.1016/j.apsusc.2020.147230>.
- [90] R. Huang, R. Zhou, L. Wang, Y. Zhu, Dandelion-like CoO/Co₃O₄/Carbon Composites as Anode Materials for a High-Performance Lithium Ion Battery, *ChemistrySelect* 5 (42) (Nov. 2020) 12932–12939, <https://doi.org/10.1002/slct.202002986>.
- [91] G. Yang, S.-J. Park, MnO₂ and biomass-derived 3D porous carbon composites electrodes for high performance supercapacitor applications, *J. Alloys Compd.* 741 (Apr. 2018) 360–367, <https://doi.org/10.1016/j.jallcom.2018.01.108>.
- [92] H. Shen, X. Kong, P. Zhang, X. Song, H. Wang, Y. Zhang, In-situ hydrothermal synthesis of δ-MnO₂/soybean pod carbon and its high-performance application on supercapacitor, *J. Alloys Compd.* 853 (Feb. 2021) 157357, <https://doi.org/10.1016/j.jallcom.2020.157357>.
- [93] W. Du, et al., Biological cell template synthesis of nitrogen-doped porous hollow carbon spheres/MnO₂ composites for high-performance asymmetric supercapacitors, *Electrochim. Acta* 296 (Feb. 2019) 907–915, <https://doi.org/10.1016/j.electacta.2018.11.074>.
- [94] Y. Zhao, C.-A. Wang, Nano-network MnO₂/polyaniline composites with enhanced electrochemical properties for supercapacitors, *Mater. Des.* 97 (May 2016) 512–518, <https://doi.org/10.1016/j.matedes.2016.02.120>.
- [95] W. Liu, et al., Fabrication of ternary hierarchical nanofibers MnO₂/PANI/CNT and theirs application in electrochemical supercapacitors, *Chem. Eng. Sci.* 156 (Dec. 2016) 178–185, <https://doi.org/10.1016/j.ces.2016.09.025>.
- [96] S. Grover, V. Sahu, G. Singh, R.K. Sharma, High specific energy ternary nanocomposite polyaniline: Manganese dioxide@ MWNT electrode for asymmetric supercapacitor, *J. Energy Storage* 29 (Jun. 2020) 101411, <https://doi.org/10.1016/j.est.2020.101411>.
- [97] X. Li, et al., Rational preparation of ternary carbon cloth/MnO₂/polyaniline nanofibers for high-performance electrochemical supercapacitors, *J. Mater. Sci. Mater. Electron.* 33 (4) (Feb. 2022) 1918–1929, <https://doi.org/10.1007/s10854-021-07393-1>.
- [98] C. Pan, H. Gu, L. Dong, Synthesis and electrochemical performance of polyaniline @MnO₂/graphene ternary composites for electrochemical supercapacitors, *J. Power Sources* 303 (Jan. 2016) 175–181, <https://doi.org/10.1016/j.jpowsour.2015.11.002>.
- [99] C. Yin, H. Zhou, J. Li, Facile one-step hydrothermal synthesis of PEDOT:PSS/MnO₂ nanorod hybrids for high-rate supercapacitor electrode materials, *Ionics* 25 (2) (Feb. 2019) 685–695, <https://doi.org/10.1007/s11581-018-2680-6>.
- [100] G. Wee, H.Z. Soh, Y.L. Cheah, S.G. Mhaisalkar, M. Srinivasan, Synthesis and electrochemical properties of electrospun V₂O₅ nanofibers as supercapacitor electrodes, *J. Mater. Chem.* 20 (32) (2010) 6720, <https://doi.org/10.1039/c0jm00059k>.
- [101] T. Wang, H.C. Chen, F. Yu, X.S. Zhao, H. Wang, Boosting the cycling stability of transition metal compounds-based supercapacitors, *Energy Storage Mater.* 16 (Jan. 2019) 545–573, <https://doi.org/10.1016/j.ensm.2018.09.007>.
- [102] Y. Ningyi, L. Jinhua, L. Chengli, Valence reduction process from sol-gel V₂O₅ to VO₂ thin films, *Appl. Surf. Sci.* 191 (1–4) (May 2002) 176–180, [https://doi.org/10.1016/S0169-4332\(02\)00180-0](https://doi.org/10.1016/S0169-4332(02)00180-0).
- [103] S. Beke, A review of the growth of V₂O₅ films from 1885 to 2010, *Thin Solid Films* 519 (6) (Jan. 2011) 1761–1771, <https://doi.org/10.1016/j.tsf.2010.11.001>.
- [104] R. Taniki I. Honma “Mg Secondary Batteries Using Nano-Crystalline V₂O₅”, *ECS Meet. Abstr.* vol. MA2016-02, no. 5 Sep. 2016 717 10.1149/MA2016-02/5/717.
- [105] X. Gao, et al., Cover Picture: Boosting High-Rate Lithium Storage of V₂O₅ Nanowires by Self-Assembly on N-Doped Graphene Nanosheets (*ChemElectroChem* 11/2016), *ChemElectroChem* 3 (11) (Nov. 2016) 1727, <https://doi.org/10.1002/celec.201600596>.
- [106] J.S. Daubert, et al., Effect of Meso- and Micro-Porosity in Carbon electrodes on atomic layer deposition of pseudocapacitive V₂O₅ for high performance supercapacitors, *Chem. Mater.* 27 (19) (Oct. 2015) 6524–6534, <https://doi.org/10.1021/acs.chemmater.5b01602>.
- [107] Q. Qu, Y. Zhu, X. Gao, Y. Wu, Core-Shell Structure of Polypyrrole Grown on V₂O₅ nanoribbon as high performance anode material for supercapacitors, *Adv. Energy Mater.* 2 (8) (Aug. 2012) 950–955, <https://doi.org/10.1002/aenm.201200088>.
- [108] K. Liang, X. Tang, W. Hu, High-performance three-dimensional nanoporous NiO film as a supercapacitor electrode, *J. Mater. Chem.* 22 (22) (2012) 11062, <https://doi.org/10.1039/c2jm31526b>.
- [109] J. Zhu, et al., Building 3D structures of vanadium pentoxide nanosheets and application as electrodes in supercapacitors, *Nano Lett.* 13 (11) (Nov. 2013) 5408–5413, <https://doi.org/10.1021/nl402969r>.
- [110] E. Uchaker, Y.Z. Zheng, S. Li, S.L. Candelaria, S. Hu, G.Z. Cao, Better than crystalline: amorphous vanadium oxide for sodium-ion batteries, *J. Mater. Chem. A* 2 (43) (Sep. 2014) 18208–18214, <https://doi.org/10.1039/C4TA03788J>.
- [111] A. Qian, K. Zhuo, M.S. Shin, W.W. Chun, B.N. Choi, C. Chung, Surfactant Effects on the Morphology and Pseudocapacitive Behavior of V₂O₅H₂O, *ChemSusChem* 8 (14) (Jul. 2015) 2399–2406, <https://doi.org/10.1002/cssc.201403477>.
- [112] J. Zheng, Y. Zhang, T. Hu, T. Lv, C. Meng, New Strategy for the Morphology-Controlled Synthesis of V₂O₅ microcrystals with enhanced capacitance as battery-type supercapacitor electrodes, *Cryst. Growth Des.* 18 (9) (Sep. 2018) 5365–5376, <https://doi.org/10.1021/acs.cgd.Bb00776>.
- [113] M.-H. Bai, T.-Y. Liu, F. Luan, Y. Li, X.-X. Liu, Electrodeposition of vanadium oxide-polyaniline composite nanowire electrodes for high energy density supercapacitors, *J. Mater. Chem. A* 2 (28) (2014) 10882–10888, <https://doi.org/10.1039/C3TA15391F>.
- [114] P. Asen, S. Shahrokhan, A. Iraji Zad, One step electrodeposition of V₂O₅/polypyrrole/graphene oxide ternary nanocomposite for preparation of a high performance supercapacitor, *Int. J. Hydrog. Energy* 42 (33) (Aug. 2017) 21073–21085, <https://doi.org/10.1016/j.ijhydene.2017.07.008>.
- [115] W. Bi, et al., Gradient Oxygen Vacancies in V₂O₅/PEDOT Nanocables for High-Performance Supercapacitors, *ACS Appl. Energy Mater.* 2 (1) (Jan. 2019) 668–677, <https://doi.org/10.1021/acsae.8B01676>.
- [116] M.M. Sk, C.Y. Yue, K. Ghosh, R.K. Jena, Review on advances in porous nanostructured nickel oxides and their composite electrodes for high-performance supercapacitors, *J. Power Sources* 308 (Mar. 2016) 121–140, <https://doi.org/10.1016/j.jpowsour.2016.01.056>.
- [117] H. Xiao, S. Yao, H. Liu, F. Qu, X. Zhang, X. Wu, NiO nanosheet assemblies for supercapacitor electrode materials, *Prog. Nat. Sci. Mater. Int.* 26 (3) (Jun. 2016) 271–275, <https://doi.org/10.1016/j.pnsc.2016.05.007>.
- [118] Q. Lu, et al., “Cover Picture: Supercapacitor Electrodes with High-Energy and Power Densities Prepared from Monolithic NiO/Ni Nanocomposites (*Angew. Chem. Int. Ed.* 30/2011),” *Angew. Chem. Int. Ed.*, vol. 50, no. 30, pp. 6673–6673, Jul. 2011, doi: 10.1002/anie.201103449.
- [119] H. Wang, H.S. Caslongue, Y. Liang, H. Dai, Ni(OH)₂ Nanoplates grown on graphene as advanced electrochemical pseudocapacitor materials, *J. Am. Chem. Soc.* 132 (21) (Jun. 2010) 7472–7477, <https://doi.org/10.1021/ja102267>.
- [120] X. Xia, et al., Graphene Sheet/Porous NiO Hybrid Film for supercapacitor applications, *Chem. – Eur. J.* 17 (39) (Sep. 2011) 10898–10905, <https://doi.org/10.1002/chem.201100727>.
- [121] F. Liu, X. Wang, J. Hao, S. Han, J. Lian, Q. Jiang, High Density Arrayed Ni/NiO Core-shell Nanospheres Evenly Distributed on Graphene for ultrahigh performance supercapacitor, *Sci. Rep.* 7 (1) (Dec. 2017) 17709, <https://doi.org/10.1038/s41598-017-17899-6>.
- [122] B.S. Singu, S. Palaniappan, K.R. Yoon, Polyaniline-nickel oxide nanocomposites for supercapacitor, *J. Appl. Electrochem.* 46 (10) (Oct. 2016) 1039–1047, <https://doi.org/10.1007/s10800-016-0988-3>.
- [123] J. Zhang, et al., Preparation of inflorescence-like ACNF/PANI/NiO composite with three-dimension nanostructure for high performance supercapacitors, *J. Electroanal. Chem.* 790 (Apr. 2017) 40–49, <https://doi.org/10.1016/j.jelechem.2017.02.047>.
- [124] E.-C. Cho, et al., Spray-dried nanoporous NiO/PANI:PSS composite microspheres for high-performance asymmetric supercapacitors, *Compos. Part B Eng.* 175 (Oct. 2019) 107066, <https://doi.org/10.1016/j.compositesb.2019.107066>.
- [125] H. Yang, H. Xu, M. Li, L. Zhang, Y. Huang, X. Hu, Assembly of NiO/Ni(OH)₂/PEDOT Nanocomposites on Contra Wires for Fiber-Shaped flexible asymmetric supercapacitors, *ACS Appl. Mater. Interfaces* 8 (3) (Jan. 2016) 1774–1779, <https://doi.org/10.1021/acsami.5b09526>.
- [126] K. Han, Y. Liu, H. Huang, Q. Gong, Z. Zhang, G. Zhou, Tremella-like NiO microspheres embedded with fish-scale-like polypyrrole for high-performance asymmetric supercapacitor, *RSC Adv.* 9 (38) (2019) 21608–21615, <https://doi.org/10.1039/C9RA03046H>.
- [127] J.P. Zheng, T.R. Jow, A New Charge Storage Mechanism for Electrochemical Capacitors, *J. Electrochem. Soc.* 142 (1) (Jan. 1995) L6–L8, <https://doi.org/10.1149/1.2043984>.
- [128] B.-O. Park, C.D. Lokhande, H.-S. Park, K.-D. Jung, O.-S. Joo, Performance of supercapacitor with electrodeposited ruthenium oxide film electrodes—effect of film thickness, *J. Power Sources* 134 (1) (Jul. 2004) 148–152, <https://doi.org/10.1016/j.jpowsour.2004.02.027>.
- [129] V.D. Patake, C.D. Lokhande, O.S. Joo, Electrodeposited ruthenium oxide thin films for supercapacitor: Effect of surface treatments, *Appl. Surf. Sci.* 255 (7) (Jan. 2009) 4192–4196, <https://doi.org/10.1016/j.apsusc.2008.11.005>.
- [130] Y.-G. Wang, Z.-D. Wang, Y.-Y. Xia, An asymmetric supercapacitor using RuO₂/TiO₂ nanotube composite and activated carbon electrodes, *Electrochim. Acta* 50 (28) (Sep. 2005) 5641–5646, <https://doi.org/10.1016/j.jelectacta.2005.03.042>.
- [131] C.-C. Hu, C.-C. Wang, K.-H. Chang, A comparison study of the capacitive behavior for sol-gel-derived and co-annealed ruthenium-tin oxide composites, *Electrochim. Acta* 52 (7) (Feb. 2007) 2691–2700, <https://doi.org/10.1016/j.jelectacta.2006.09.026>.

- [132] H. Kim, B.N. Popov, Characterization of hydrous ruthenium oxide/carbon nanocomposite supercapacitors prepared by a colloidal method, *J. Power Sources* 104 (1) (Jan. 2002) 52–61, [https://doi.org/10.1016/S0378-7753\(01\)00903-X](https://doi.org/10.1016/S0378-7753(01)00903-X).
- [133] M. Dandekar, G. Arabale, K. Vijayamohanan, Preparation and characterization of composite electrodes of coconut-shell-based activated carbon and hydrous ruthenium oxide for supercapacitors, *J. Power Sources* 141 (1) (Feb. 2005) 198–203, <https://doi.org/10.1016/j.jpowsour.2004.09.008>.
- [134] U.M. Patil, K.V. Gurav, V.J. Fulari, C.D. Lokhande, O.-S. Joo, Characterization of honeycomb-like ‘ β -Ni(OH)₂’ thin films synthesized by chemical bath deposition method and their supercapacitor application, *J. Power Sources* 188 (1) (Mar. 2009) 338–342, <https://doi.org/10.1016/j.jpowsour.2008.11.136>.
- [135] U.M. Patil, R.R. Salunkhe, K.V. Gurav, C.D. Lokhande, Chemically deposited nanocrystalline NiO thin films for supercapacitor application, *Appl. Surf. Sci.* 255 (5) (Dec. 2008) 2603–2607, <https://doi.org/10.1016/j.apsusc.2008.07.192>.
- [136] S.B. Kulkarni, V.S. Jamadade, D.S. Dhawale, C.D. Lokhande, Synthesis and characterization of β -Ni(OH)₂ up grown nanoflakes by SILAR method, *Appl. Surf. Sci.* 255 (20) (Jul. 2009) 8390–8394, <https://doi.org/10.1016/j.apsusc.2009.05.095>.
- [137] K.-W. Nam, K.-B. Kim, A Study of the Preparation of NiO[sub x] electrode via electrochemical route for supercapacitor applications and their charge storage mechanism, *J. Electrochem. Soc.* 149 (3) (2002) A346, <https://doi.org/10.1149/1.1449951>.
- [138] X.M. Liu, X.G. Zhang, NiO-based composite electrode with RuO₂ for electrochemical capacitors, *Electrochim. Acta* 49 (2) (Jan. 2004) 229–232, <https://doi.org/10.1016/j.electacta.2003.08.005>.
- [139] M. Wu, J. Gao, S. Zhang, A. Chen, Synthesis and characterization of aerogel-like mesoporous nickel oxide for electrochemical supercapacitors, *J. Porous Mater.* 13 (3–4) (Aug. 2006) 407–412, <https://doi.org/10.1007/s10934-006-8038-x>.
- [140] Z. Fan, J. Chen, K. Cui, F. Sun, Y. Xu, Y. Kuang, Preparation and capacitive properties of cobalt–nickel oxides/carbon nanotube composites, *Electrochim. Acta* 52 (9) (Feb. 2007) 2959–2965, <https://doi.org/10.1016/j.electacta.2006.09.029>.
- [141] D.-D. Zhao, S.-J. Bao, W.-J. Zhou, H.-L. Li, Preparation of hexagonal nanoporous nickel hydroxide film and its application for electrochemical capacitor, *Electrochim. Commun.* 9 (5) (May 2007) 869–874, <https://doi.org/10.1016/j.electcom.2006.11.030>.
- [142] Y. Wang, Y. Xia, Electrochemical capacitance characterization of NiO with ordered mesoporous structure synthesized by template SBA-15, *Electrochim. Acta* 51 (16) (Apr. 2006) 3223–3227, <https://doi.org/10.1016/j.electacta.2005.09.013>.
- [143] Y. Gao, S. Chen, D. Cao, G. Wang, J. Yin, Electrochemical capacitance of Co₃O₄ nanowire arrays supported on nickel foam, *J. Power Sources* 195 (6) (Mar. 2010) 1757–1760, <https://doi.org/10.1016/j.jpowsour.2009.09.048>.
- [144] S.G. Kandalkar, J.L. Gunjakar, C.D. Lokhande, Preparation of cobalt oxide thin films and its use in supercapacitor application, *Appl. Surf. Sci.* 254 (17) (Jun. 2008) 5540–5544, <https://doi.org/10.1016/j.apsusc.2008.02.163>.
- [145] C.-K. Min, T.-B. Wu, W.-T. Yang, C.-L. Li, Nanocrystalline ruthenium oxide of fine mesoporosity prepared by templating for electrochemical capacitor applications, *Mater. Chem. Phys.* 117 (1) (Sep. 2009) 70–73, <https://doi.org/10.1016/j.matchemphys.2009.05.011>.
- [146] G.-Y. Zhao, C.-L. Xu, H.-L. Li, Highly ordered cobalt–manganese oxide (CMO) nanowire array thin film on Ti/Si substrate as an electrode for electrochemical capacitor, *J. Power Sources* 163 (2) (Jan. 2007) 1132–1136, <https://doi.org/10.1016/j.jpowsour.2006.09.085>.
- [147] K. Rajendra Prasad, N. Miura, Electrochemically synthesized MnO₂-based mixed oxides for high performance redox supercapacitors, *Electrochim. Commun.* 6 (10) (Oct. 2004) 1004–1008, <https://doi.org/10.1016/j.electcom.2004.07.017>.
- [148] V.R. Shinde, S.B. Mahadik, T.P. Gujar, C.D. Lokhande, Supercapacitive cobalt oxide (Co₃O₄) thin films by spray pyrolysis, *Appl. Surf. Sci.* 252 (20) (Aug. 2006) 7487–7492, <https://doi.org/10.1016/j.apsusc.2005.09.004>.
- [149] A.A.F. Grupioni, E. Arashiro, T.A.F. Lassali, Voltammetric characterization of an iridium oxide-based system: the pseudocapacitive nature of the Ir_{0.3}Mn_{0.7}O₂ electrode, *Electrochim. Acta* 48 (4) (Dec. 2002) 407–418, [https://doi.org/10.1016/S0013-4686\(02\)00686-2](https://doi.org/10.1016/S0013-4686(02)00686-2).
- [150] S. Chen, J. Zhu, X. Wu, Q. Han, X. Wang, Graphene Oxide–MnO₂ Nanocomposites for Supercapacitors, *ACS Nano* 4 (5) (May 2010) 2822–2830, <https://doi.org/10.1021/nn901311t>.
- [151] M.S. Yadav, S.K. Tripathi, Synthesis and characterization of nanocomposite NiO/activated charcoal electrodes for supercapacitor application, *Ionics* 23 (10) (Oct. 2017) 2919–2930, <https://doi.org/10.1007/s11581-017-2026-9>.
- [152] M.S. Yadav, N. Singh, S.M. Bobade, Zinc oxide nanoparticles and activated charcoal-based nanocomposite electrode for supercapacitor application, *Ionics* 24 (11) (Nov. 2018) 3611–3630, <https://doi.org/10.1007/s11581-018-2527-1>.
- [153] M.S. Yadav, N. Singh, S.M. Bobade, V_xO_y nanoparticles and activated charcoal based nanocomposite for supercapacitor electrode application, *Ionics* 26 (5) (May 2020) 2581–2598, <https://doi.org/10.1007/s11581-019-03345-2>.
- [154] K.-W. Nam, W.-S. Yoon, K.-B. Kim, X-ray absorption spectroscopy studies of nickel oxide thin film electrodes for supercapacitors, *Electrochim. Acta* 47 (19) (Jul. 2002) 3201–3209, [https://doi.org/10.1016/S0013-4686\(02\)00240-2](https://doi.org/10.1016/S0013-4686(02)00240-2).
- [155] F. Naeem, et al., Atomic layer deposition synthesized ZnO nanomembranes: a facile route towards stable supercapacitor electrode for high capacitance, *J. Power Sources* 451 (Mar. 2020) 227740, <https://doi.org/10.1016/j.jpowsour.2020.227740>.
- [156] R.M. Obodo, et al., Evaluation of 8.0 MeV Carbon (C 2+) Irradiation Effects on Hydrothermally Synthesized Co 3 O 4 –CuO–ZnO@GO electrodes for supercapacitor applications, *Electroanalysis* 32 (12) (Dec. 2020) 2958–2968, <https://doi.org/10.1002/elan.202060382>.
- [157] M. Miah, T.K. Mondal, A. Ghosh, S.K. Saha, Study of highly porous ZnO nanospheres embedded reduced graphene oxide for high performance supercapacitor application, *Electrochim. Acta* 354 (Sep. 2020) 136675, <https://doi.org/10.1016/j.electacta.2020.136675>.
- [158] T.P. Gujar, V.R. Shinde, C.D. Lokhande, W.-Y. Kim, K.-D. Jung, O.-S. Joo, Spray deposited amorphous RuO₂ for an effective use in electrochemical supercapacitor, *Electrochim. Commun.* 9 (3) (Mar. 2007) 504–510, <https://doi.org/10.1016/j.elecom.2006.10.017>.
- [159] Y. Zhu, H. Xu, P. Chen, Y. Bao, X. Jiang, Y. Chen, Electrochemical performance of polyaniline-coated γ -MnO₂ on carbon cloth as flexible electrode for supercapacitor, *Electrochim. Acta* 413 (May 2022) 140146, <https://doi.org/10.1016/j.electacta.2022.140146>.
- [160] C. Huang, et al., Synthesis of polyaniline/nickel oxide/sulfonated graphene ternary composite for all-solid-state asymmetric supercapacitor, *Appl. Surf. Sci.* 505 (Mar. 2020) 144589, <https://doi.org/10.1016/j.apsusc.2019.144589>.
- [161] Y. Fan, H. Chen, Y. Li, D. Cui, Z. Fan, C. Xue, PANI-Co₃O₄ with excellent specific capacitance as an electrode for supercapacitors, *Ceram. Int.* 47 (6) (Mar. 2021) 8433–8440, <https://doi.org/10.1016/j.ceramint.2020.11.208>.
- [162] K. Chhetri, et al., A ZIF-8-derived nanoporous carbon nanocomposite wrapped with Co₃O₄-polyaniline as an efficient electrode material for an asymmetric supercapacitor, *J. Electroanal. Chem.* 856 (Jan. 2020) 113670, <https://doi.org/10.1016/j.jelechem.2019.113670>.
- [163] W.-J. Zhuo, Y.-H. Wang, C.-T. Huang, M.-J. Deng, Enhanced Pseudocapacitive Performance of Symmetric Polyppyrrole-MnO₂ Electrode and Polymer Gel Electrolyte, *Polymers* 13 (20) (Oct. 2021) 3577, <https://doi.org/10.3390/polym13203577>.
- [164] J. Jyothibus, et al., V₂O₅/Carbon Nanotube/Polyppyrrole Based freestanding negative electrodes for high-performance supercapacitors, *Catalysts* 11 (8) (Aug. 2021) 980, <https://doi.org/10.3390/catal11080980>.
- [165] J. Xue, et al., High-performance ordered porous Polypyrrole/ZnO films with improved specific capacitance for supercapacitors, *Mater. Chem. Phys.* 256 (Dec. 2020) 123591, <https://doi.org/10.1016/j.matchemphys.2020.123591>.
- [166] Z.-M. Shen, X.-J. Luo, Y.-Y. Zhu, Y.-S. Liu, Facile co-deposition of NiO-CoO-PPy composite for asymmetric supercapacitors, *J. Energy Storage* 51 (Jul. 2022) 104475, <https://doi.org/10.1016/j.est.2022.104475>.
- [167] R. Ravit, N.H.N. Azman, S. Kulandaivelu, I. Abdullah, I. Ahmad, Y. Sulaiman, Cauliflower-like poly(3,4-ethylenedioxothiophene)/nanocrystalline cellulose/manganese oxide ternary nanocomposite for supercapacitor, *J. Appl. Polym. Sci.* 137 (39) (Oct. 2020) 49162, <https://doi.org/10.1002/app.49162>.
- [168] L. Wang, et al., Fabricating strongly coupled V₂O₅@PEDOT nanobelts/graphene hybrid films with high areal capacitance and facile transferability for transparent solid-state supercapacitors, *Energy Storage Mater.* 27 (May 2020) 150–158, <https://doi.org/10.1016/j.ensm.2020.01.026>.
- [169] N. H. Nabilah Azman and Y. Sulaiman, “Supercapattery performance of carbon nanofibers decorated with poly(3,4-ethylenedioxothiophene) and cobalt oxide,” *Ceram. Int.*, vol. 48, no. 8, pp. 11772–11778, Apr. 2022, doi: 10.1016/j.ceramint.2022.01.036.
- [170] G. Liu, L. Ma, Q. Liu, The preparation of Co₃O₄@MnO₂ hierarchical nano-sheets for high-output potential supercapacitors, *Electrochim. Acta* 364 (Dec. 2020) 137265, <https://doi.org/10.1016/j.electacta.2020.137265>.
- [171] S. Arunpandiyan, S. Bharathi, A. Pandikumar, S. Ezhil Arasi, and A. Arivarasan, “Structural analysis and redox additive electrolyte based supercapacitor performance of ZnO/Ce_{0.2} nanocomposite,” *Mater. Sci. Semicond. Process.*, vol. 106, p. 104765, Feb. 2020, doi: 10.1016/j.mssp.2019.104765.
- [172] S.-H. Ji, N.R. Chodankar, D.-H. Kim, Aqueous asymmetric supercapacitor based on RuO₂-WO₃ electrodes, *Electrochim. Acta* 325 (Dec. 2019) 134879, <https://doi.org/10.1016/j.electacta.2019.134879>.
- [173] K. Xu, et al., Hierarchical mesoporous NiCo₂O₄@MnO₂ core–shell nanowire arrays on nickel foam for aqueous asymmetric supercapacitors, *J. Mater. Chem. A* 2 (13) (2014) 4795, <https://doi.org/10.1039/c3ta14647b>.
- [174] M. Ramani, B.S. Haran, R.E. White, B.N. Popov, Synthesis and Characterization of Hydrous Ruthenium Oxide-Carbon Supercapacitors, *J. Electrochim. Soc.* 148 (4) (2001) A374, <https://doi.org/10.1149/1.1357172>.
- [175] N.-L. Wu, S.-L. Kuo, M.-H. Lee, Preparation and optimization of RuO₂-impregnated SnO₂ xerogel supercapacitor, *J. Power Sources* 104 (1) (Jan. 2002) 62–65, [https://doi.org/10.1016/S0378-7753\(01\)00873-4](https://doi.org/10.1016/S0378-7753(01)00873-4).
- [176] C.-C. Hu, W.-C. Chen, K.-H. Chang, How to achieve maximum utilization of hydrous ruthenium oxide for supercapacitors, *J. Electrochim. Soc.* 151 (2) (2004) A281, <https://doi.org/10.1149/1.1639020>.
- [177] C.-C. Hu, K.-H. Chang, M.-C. Lin, Y.-T. Wu, Design and Tailoring of the Nanotubular Arrayed Architecture of Hydrous RuO₂ for Next Generation Supercapacitors, *Nano Lett.* 6 (12) (Dec. 2006) 2690–2695, <https://doi.org/10.1021/nl061576a>.
- [178] H. Ma, et al., Disassembly–Reassembly Approach to RuO₂/Graphene composites for ultrahigh volumetric capacitance supercapacitor, *Small* 13 (30) (Aug. 2017) 1701026, <https://doi.org/10.1002/smll.201701026>.
- [179] S.-C. Pang, M.A. Anderson, T.W. Chapman, Novel Electrode Materials for Thin-Film Ultracapacitors: comparison of electrochemical properties of Sol-Gel-Derived and electrodeposited manganese dioxide, *J. Electrochim. Soc.* 147 (2) (2000) 444, <https://doi.org/10.1149/1.1393216>.
- [180] M. Toupin, T. Brousse, D. Bélanger, Influence of Microstructure on the Charge Storage Properties of Chemically Synthesized Manganese Dioxide, *Chem. Mater.* 14 (9) (Sep. 2002) 3946–3952, <https://doi.org/10.1021/cm020408q>.

- [181] V. Subramanian, H. Zhu, R. Vajtai, P.M. Ajayan, B. Wei, Hydrothermal Synthesis and Pseudocapacitance Properties of MnO₂ Nanostructures, *J. Phys. Chem. B* 109 (43) (Nov. 2005) 20207–20214, <https://doi.org/10.1021/jp0543330>.
- [182] S. Devaraj, N. Munichandraiah, Effect of Crystallographic Structure of MnO₂ on Its Electrochemical Capacitance Properties, *J. Phys. Chem. C* 112 (11) (Mar. 2008) 4406–4417, <https://doi.org/10.1021/jp7108785>.
- [183] T.D. Dongale, P.R. Jadhav, G.J. Navathe, J.H. Kim, M.M. Karanjkar, P.S. Patil, Development of nano fiber MnO₂ thin film electrode and cyclic voltammetry behavior modeling using artificial neural network for supercapacitor application, *Mater. Sci. Semicond. Process.* 36 (Aug. 2015) 43–48, <https://doi.org/10.1016/j.mssp.2015.02.084>.
- [184] X. Zhang, et al., Synthesis of porous NiO nanocrystals with controllable surface area and their application as supercapacitor electrodes, *Nano Res.* 3 (9) (Sep. 2010) 643–652, <https://doi.org/10.1007/s12274-010-0024-6>.
- [185] F. Miao, B. Tao, P. Ci, J. Shi, L. Wang, P.K. Chu, 3D ordered NiO/silicon MCP array electrode materials for electrochemical supercapacitors, *Mater. Res. Bull.* 44 (9) (Sep. 2009) 1920–1925, <https://doi.org/10.1016/j.materresbull.2009.05.004>.
- [186] X. Xia, J. Tu, X. Wang, C. Gu, X. Zhao, Hierarchically porous NiO film grown by chemical bath deposition via a colloidal crystal template as an electrochemical pseudocapacitor material, *J Mater Chem* 21 (3) (2011) 671–679, <https://doi.org/10.1039/C0JM02784G>.
- [187] S. Zhu, et al., In situ preparation of NiO nanoflakes on Ni foams for high performance supercapacitors, *Mater. Lett.* 161 (Dec. 2015) 731–734, <https://doi.org/10.1016/j.matlet.2015.09.086>.
- [188] Q. Hu, Z. Gu, X. Zheng, X. Zhang, Three-dimensional Co₃O₄@NiO hierarchical nanowire arrays for solid-state symmetric supercapacitor with enhanced electrochemical performances, *Chem. Eng. J.* 304 (Nov. 2016) 223–231, <https://doi.org/10.1016/j.cej.2016.06.097>.
- [189] Y. Ouyang, et al., Three-Dimensional Hierarchical Structure ZnO@C@NiO on carbon cloth for asymmetric supercapacitor with enhanced cycle stability, *ACS Appl. Mater. Interfaces* 10 (4) (Jan. 2018) 3549–3561, <https://doi.org/10.1021/acsami.7b16021>.
- [190] A. Bello, K. Makgopa, M. Fabiane, D. Dodoo-Ahrin, K.I. Ozoemena, N. Manyala, Chemical adsorption of NiO nanostructures on nickel foam-graphene for supercapacitor applications, *J. Mater. Sci.* 48 (19) (Oct. 2013) 6707–6712, <https://doi.org/10.1007/s10853-013-7471-x>.
- [191] P.E. Lokhande, U.S. Chavan, Nanoflower-like Ni(OH)₂ synthesis with chemical bath deposition method for high performance electrochemical applications, *Mater. Lett.* 218 (May 2018) 225–228, <https://doi.org/10.1016/j.matlet.2018.02.012>.
- [192] Y. Xi, et al., Facile synthesis of MnO₂-Ni(OH)₂ 3D Ridge-like Porous electrode materials by seed-induce method for high-performance asymmetric supercapacitor, *Electrochim. Acta* 233 (Apr. 2017) 26–35, <https://doi.org/10.1016/j.electacta.2017.02.038>.
- [193] X. Bai, et al., Hierarchical Co 3 O 4 @Ni(OH)₂ core-shell nanosheet arrays for isolated all-solid state supercapacitor electrodes with superior electrochemical performance, *Chem. Eng. J.* 315 (May 2017) 35–45, <https://doi.org/10.1016/j.cej.2017.01.010>.
- [194] J. Hao, X. Wang, F. Liu, S. Han, J. Lian, Q. Jiang, Facile Synthesis ZnS/ZnO/Ni(OH)₂ Composites Grown on Ni Foam: a bifunctional materials for photocatalysts and supercapacitors, *Sci. Rep.* 7 (1) (Jun. 2017) 3021, <https://doi.org/10.1038/s41598-017-03200-2>.
- [195] S. Kong, et al., MnO₂ nanosheets decorated porous active carbon derived from wheat bran for high-performance asymmetric supercapacitor, *J. Electroanal. Chem.* 850 (Oct. 2019) 113412, <https://doi.org/10.1016/j.jelechem.2019.113412>.
- [196] M. Dirican, M. Yanilmaz, A.M. Asiri, X. Zhang, Polyaniline/MnO₂/porous carbon nanofiber electrodes for supercapacitors, *J. Electroanal. Chem.* 861 (Mar. 2020) 113995, <https://doi.org/10.1016/j.jelechem.2020.113995>.
- [197] P. Periasamy, et al., Preparation and comparison of hybridized WO₃–V2O₅ nanocomposites electrochemical supercapacitor performance in KOH and H₂SO₄ electrolyte, *Mater. Lett.* 236 (Feb. 2019) 702–705, <https://doi.org/10.1016/j.matlet.2018.11.050>.
- [198] H. Chen, et al., Facile synthesis of 3D gem shape Co₃O₄ with mesoporous structure as electrode for high-performance supercapacitors, *J. Alloys Compd.* 819 (Apr. 2020) 152939, <https://doi.org/10.1016/j.jallcom.2019.152939>.